ELSEVIER

Bicyclic peptidomimetic tetrahydrofuro[3,2-*b*]pyrrol-3-one and hexahydrofuro[3,2-*b*]pyridine-3-one based scaffolds: synthesis and cysteinyl proteinase inhibition

Martin Quibell,* Alex Benn, Nick Flinn, Tracy Monk, Manoj Ramjee, Yikang Wang and John Watts

Amura Therapeutics Limited, Incenta House, Horizon Park, Barton Road, Comberton, Cambridge CB3 7AJ, UK

Abstract—A stereoselective synthesis of (3a*S*,6a*R*)-tetrahydrofuro[3,2-*b*]pyrrol-3-ones and (3a*S*,7a*R*)-hexahydrofuro[3,2-*b*]pyridine-3-ones has been developed through Fmoc protected scaffolds **12** and **13**. A key design element within these novel bicyclic scaffolds, in particular the 5,5-fused system, was the inherent stability of the *cis*-fused geometry in comparison to that of the corresponding *trans*-fused. Since the bridgehead stereocentre situated β to the ketone was of a fixed and stable configuration, the fact that *cis* ring fusion is both kinetically and thermodynamically stable with respect to *trans* ring fusion provides chiral stability to the bridgehead stereocentre that is situated α to the ketone. To exemplify this principle, building blocks **12** and **13** were designed, prepared and utilised in a solid phase combinatorial synthesis of peptidomimetic inhibitors **10**, **45a**–**e**, **11** and **46**. Both series were chirally stable with 5,5-series **10** and **45a**–**e** exhibiting potent in vitro activity against a range of CAC1 cysteinyl proteinases. Compound **10**, a potent and selective inhibitor of cathepsin K, possessed good primary DMPK properties along with promising activity in an in vitro cell-based human osteoclast assay of bone resorption.
© 2004 Elsevier Ltd. All rights reserved.

1. Introduction

The therapeutic control of disease-associated cysteinyl proteinase activity represents a hitherto unexploited area of tremendous medical and commercial potential.[1] In particular, the last decade has seen the biology of human cysteinyl proteinase function develop enormously[2] and as a consequence there has been a concerted drive within the pharmaceutical industry towards the development of inhibitors of this class of proteinase that are suitable for human administration.[3,4] Previously, we have detailed our studies concerning the synthesis and activity of 2,3-dimethyl-3-amino-tetrahydrofuran-4-one **1** and *N*-(3-oxo-hexahydrocyclopenta[*b*]furan-3*a*-yl)acylamide **2** based scaffolds as general templates towards the inhibition of clan CA/family C1 (CAC1) cysteinyl proteinases.[3,5] A key design element built into scaffolds **1** and **2** was the removal of

the enolisable α-proton through the introduction of an α-alkyl group at monocyclic ring position 3 or bicyclic ring position 3a. α-Alkylation provided chiral stability into the otherwise configurationally unstable keto-containing five-membered ring **3**,[6] which is a physiochemical characteristic that has hindered the pre-clinical development of inhibitor series **3**.[6c]

**1** (2*R* or *S*, 3*R*)   **2** (3*aR*, 6*aR*)   **3**
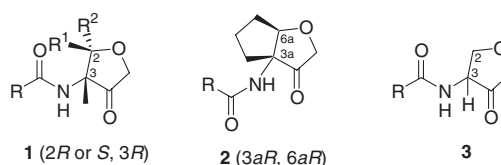
Our previous studies highlighted that inhibitors based upon scaffolds **1** and **2**, although now chirally stable, generally suffered from a greater than 10-fold loss in potency when compared to the corresponding nonalpha alkylated analogue **3**.[5] Upon closer examination of the proteinase-inhibitor kinetics, we observed that analogues of **1** and **2** exhibited broadly similar off-rates

(k_{off})[7] when compared to the corresponding analogue **3**. However, **1** and **2** were found to exhibit on-rates (k_{on}) that were greater than 40-fold slower when compared with **3** and this was the major contributing factor towards the substantial loss in potency. Therefore, we have sought alternatives to the α-alkylation approach to stabilise the α-chiral centre, to provide scaffolds that do not suffer from a dramatic slowing of the proteinase-inhibitor on-rate and thus retain the attractive potency of series **3**. Herein we report our design strategy, building block preparation, solid phase synthesis and inhibition kinetics for a series of bicyclic peptidomimetic tetrahydrofuro[3,2-*b*]pyrrol-3-one **4** and hexahydrofuro[3,2-*b*]pyridine-3-one **5** based analogues. These bicyclic analogues exhibited similar inhibition kinetics to those of monocycle **3** and as such have utility as general templates towards the inhibition of CAC1 cysteinyl proteinases.[8]
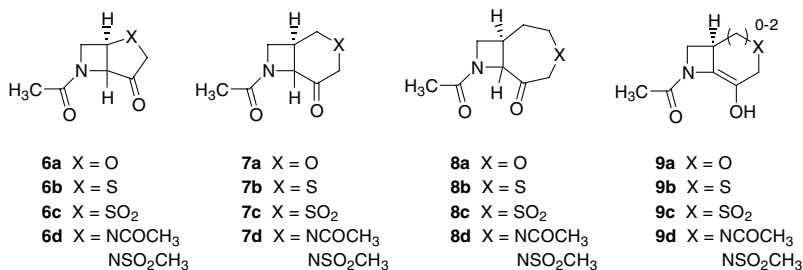

4 (3a*S*, 6a*R*)   **5** (3a*S*, 7a*R*)
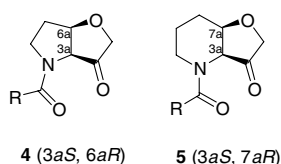
2. Results and discussion

2.1. Design strategy

Our design strategy commenced with an examination of the energetics associated with fused carbocyclic rings, a subject that has been thoroughly discussed by Eliel et al.[9] The fundamental principle behind our strategy was to identify a fused ring system where the thermodynamic stability of the *cis* and *trans*-fused geometries were substantially different and to utilise this as a basis for engineering chiral stability into a ketoheterocyclic inhibitor scaffold. Therefore, a range of fused carbocyclic rings were compared to ascertain whether *cis* and *trans*-fused examples were known (e.g., bicyclo[3.2.0]-heptane,[10a,b] bicyclo[4.2.0]octane,[10c,d] bicyclo[5.2.0]nonane,[10e] bicyclo[3.3.0]octane[10f] and bicyclo [4.3.0]-nonane[10g] and where available, literature values for the heat of combustion compiled. The literature search

octan-2-one,[11b] bicyclo[5.2.0]nonan-6-one,[11c] bicyclo-[3.3.0]octan-2-one,[12] bicyclo[4.3.0]nonan-2-one[13a–d] and general reviews of various ring fusions[13b,14a,b]). Finally, since cyclic systems containing heteroatoms *and* an α-ketone are at present virtually unknown in the literature, we performed conformer energy calculations. The calculations were first validated on the known carbocycles and ketocarbocycles by comparison to literature experimental conformational stabilities. The calculations were then repeated on our model ketoheterocyclic systems **4**–**8** as an indicator of conformer strain and potential chiral stability.[15,16]

In the 4,5-ketocarbocycle only the *cis*-fused system is known,[11a] whilst the 4,6-ketocarbocycle exists both *cis* and *trans*-fused,[11b] although the *trans* converts exclusively to the *cis* under basic conditions. The 4,7-ketocarbocycle is at present unknown.[11c] Extension of these known 4,*n*-ketocarbocycles through the addition of heteroatoms provided theoretical scaffolds 2-oxa-6-aza-bicyclo[3.2.0]heptan-4-one **6a**, 3-oxa-7-aza-bicyclo-[4.2.0]octan-5-one **7a** and 4-oxa-8-aza-bicyclo[5.2.0]-nonan-6-one **8a**. Our conformer energy calculations for **6a** and **7a** gave a substantial difference between *cis* and *trans*-fused systems, which was in agreement with the experimental findings for the corresponding 4,5- and 4,6-ketocarbocycles.[11a,b] Our calculated values gave *cis*-**6a** (43.6 kcal/mol), *trans*-**6a** (75.7 kcal/mol) and the corresponding enol intermediate **9a** at 51.2 kcal/mol and *cis*-**7a** (44.1 kcal/mol), *trans*-**7a** (59.2 kcal/mol) and the enol intermediate at 47.9 kcal/mol. These data indicated that scaffolds **6a** and **7a** have the *potential* to exhibit thermodynamic chiral stability α to the ketone because the *trans*-fused ring geometry is of a much higher energy than that of the *cis*-fused and therefore equilibrium will favour the *cis*-isomer.[11b,16] When considering theoretical scaffold **8a**, which derives from the unknown 4,7-ketocarbocycle, our calculations indicated that there *could* be thermodynamic chiral instability α to the ketone because *cis*-**8a** (48.8 kcal/mol) and *trans*-**8a** (52.4 kcal/mol) are calculated to be of approximately equal energy. However, for epimerisation to occur within any of the theoretical ketoheterocyclic systems considered, an enol intermediate containing an sp^2 hybridised bridgehead such as **9** is required, which may provide an additional transition state energy barrier to loss of chirality.

6a X = O
6b X = S
6c X = SO$_2$
6d X = NCOCH$_3$
    NSO$_2$CH$_3$

7a X = O
7b X = S
7c X = SO$_2$
7d X = NCOCH$_3$
    NSO$_2$CH$_3$

8a X = O
8b X = S
8c X = SO$_2$
8d X = NCOCH$_3$
    NSO$_2$CH$_3$

9a X = O
9b X = S
9c X = SO$_2$
9d X = NCOCH$_3$
    NSO$_2$CH$_3$

was then extended to also include carbocycles containing a ketone functionality situated α to a bridgehead carbon (e.g., bicyclo[3.2.0]heptan-2-one,[11a] bicyclo[4.2.0]-

We then considered heterocyclic rings based upon the 5,5-fused bicyclo[3.3.0]octane where literature details that the *trans* isomer is known, but has a higher heat

of combustion by approximately 6 kcal/mol compared to the *cis*-isomer,[10f] indicating the presence of substantial strain.[17] In contrast, when considering the 6,5-fused bicyclo[4.3.0]nonane, literature details that the *trans* isomer has a slightly smaller heat of combustion by approximately 1 kcal/mol compared to the *cis*-isomer.[10g] These finding are mirrored within the known 5,5- and 6,5-ketocarbocycles. Thus, bicyclo[3.3.0]octan-2-one is only known as the *cis*-isomer[12] whilst bicyclo[4.3.0]-nonan-2-one[13a–d] is known in both *cis*[13d] and *trans*[13b] ring fusions, which at equilibrium under base conditions favour a 2:1 ratio of the *cis*-isomer.[13c] Our conformer total energy calculations indicated a similar set of conclusions within the tetrahydrofuro[3,2-*b*]pyrrol-3-one **4** and hexahydrofuro[3,2-*b*]pyridine-3-one **5** ketoheterocyclic scaffolds. We calculated that *cis*-**4** (R=CH$_3$, 23.4 kcal/mol) was significantly less strained than *trans*-**4** (R=CH$_3$, 37.6 kcal/mol), whilst *cis*-**5** (R=CH$_3$, 26.3 kcal/mol) was comparatively closer in terms of total steric energy to *trans*-**5** (R=CH$_3$, 32.1 kcal/mol). Thus, in a similar manner to the conclusions drawn for scaffolds **6a**, **7a** and **8a** earlier, our calculated data indicated that scaffold **4** *could* show thermodynamic chiral stability α to the ketone because the *trans*-fused ring system is of a much higher energy when compared to that of the *cis*-fused, whereas for scaffold **5** the predicted stability is less defined.[16] As a final conclusion from the energy calculations, whilst the *cis*-fused geometries of bicycles **4**, **6a** and **7a** were predicted to be chirally stable, the 5,5-*cis*-fused bicycle **4** (R=CH$_3$, 23.4 kcal/mol) was predicted to be of a significantly lower overall strain energy compared to the 4,5-*cis*-fused bicycle **6a** (43.6 kcal/mol) and 4,6-*cis*-fused bicycle **7a** (44.1 kcal/mol). These calculations in combination with our molecular modelling studies and synthetic chemistry review detailed below, led us to choose the templates tetrahydrofuro[3,2-*b*]pyrrol-3-one **4** and hexahydrofuro[3,2-*b*]pyridine-3-one **5** to exemplify our design principles described herein towards bicyclic scaffolds for the inhibition of CAC1 cysteinyl proteinases.

Conceptually the introduction of a bicyclic scaffold that binds at the catalytic centre for the inhibition of CAC1 proteinases is in direct contrast with all other scaffolds to date that are based upon substrate-like binding modes.[1,2b,c,4b] This observation may be explained by an examination of crystal co-complexes for a whole range of CAC1 proteinases with substrate-like inhibitors, which reveal a number of conserved features. In many structures, the inhibitor P1 secondary amide NH forms a hydrogen bond with the main chain carbonyl of the proteinase residue that precedes the active site histidine.[18] However, examples also exist where this hydrogen bond is absent, for example, in a five-membered furanone,[6a] in a seven-membered azepanone,[6b] and in an acyclic peptidomimetic ketone[19] where in these cases the P1 secondary amide NH is positioned in the usual spatial orientation, but lies slightly too far from the main chain carbonyl for hydrogen bonding. The perceived importance of this inhibitor NH is clearly seen throughout the scientific and patent literature since it is conserved in all series to date. Indeed in the few reported examples where the amide has been *N*-methyl-

ated, for example, in a potent nitrile series for cathepsin B,[18f] only analogues devoid of activity were found.[20] Additionally, a range of CAC1 proteinase crystal structures containing peptidomimetic substrate-like inhibitors show the secondary amide bond of the inhibitor P2–P1 moiety in both *cis* and *trans* conformations.[21] The major additional factor here is that the orientation of the inhibitor P2–P1 secondary amide bond permits the P2 carbonyl group to accept a universally conserved hydrogen bond from a backbone NH of a proteinase glycine residue. Taking into consideration this wealth of literature precedence detailing substrate-like inhibitor design, it would appear counter-intuitive to alkylate the P1 NH and lock the inhibitor into a bicyclic scaffold, even though such a scaffold may exhibit the desired chiral stability. Nevertheless, we performed a series of molecular modelling studies utilising ketoheterocyclic scaffolds **4** and **5** examining both *si* and *re* stereofacial addition of the proteinase active site thiol to the inhibitor ketone functionality, which produced intriguing binding model predictions (Figs. 1 and 2).[22,23]

Considering the binding predictions for the 5,5-*cis*-fused analogue **10**, molecular modelling of *si* thiolate addition (Fig. 1a) predicted that the oxygen of the hemithioketal would be stabilised by a hydrogen bond to the NH$_2$ of the primary carboxamide side chain of glutamine[19] and a second hydrogen bond to the backbone NH of cysteine.[25] Additional hydrogen bonds were predicted between the P2 carbonyl oxygen of **10** and the backbone NH of glycine[66] and the P2 NH of **10** and the backbone carbonyl of glycine[66]. It was predicted that the bicycle would be puckered to give an approximately −30° dihedral angle (looking along the bond from C-6a→C-3a) between the bridgehead protons. In contrast, *re* thiolate addition to analogue **10** (Fig. 1b) was predicted to exhibit the same P2/P1 interactions as for *si* addition, however the hydroxyl of the hemithioketal was now stabilised by two hydrogen bonds from the π-NH of the imidazole side chain of histidine[159] and the bicycle would now be puckered to give an approximately +30° dihedral angle (looking along the bond from C-6a→C-3a) between the bridgehead protons. Both of these potential conformations exhibited a *cis* P2–P1 secondary amide, which has previously been observed in substrate-like inhibitors,[21] and crucially the projected angle of the P2 carbonyl was predicted to allow the conserved inhibitor—proteinase backbone hydrogen bonding network to be preserved. Thus, the overall predicted fit for analogue **10** appeared promising and we contemplated that the loss of the P1 NH hydrogen bond may be balanced by the benefits afforded by the incorporation of conformational constraint, possibly into a bioactive conformation, introduced by the bi-cyclisation process.[6b,24] We then considered the binding predictions for the 6,5-*cis*-fused analogue **11**, which gave virtually identical conclusions to those drawn for the 5,5-*cis*-fused analogue **10** (compare Fig. 1a and b with Fig. 2a and b). However, we observed that when expanding from the 5,5-*cis*-fused **10** to the 6,5-*cis*-fused **11**, the protons of the inserted methylene in the six-membered ring of **11** approached within 2 Å of the α-proton of the P2 leucine residue in both *si* and
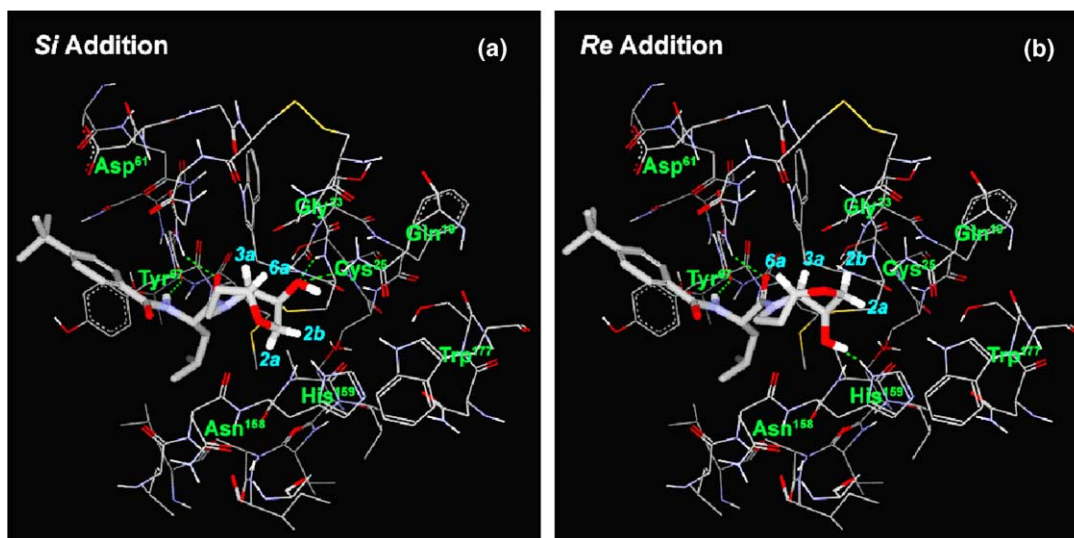
Figure 1. Predicted binding conformations for *si* (a) and *re* (b) stereofacial thiolate addition to (3aS,6aR)-4-*tert*-butyl-*N*-[3-methyl-1S-(3-oxo-hexahydrofuro[3,2-*b*]pyrrole-4-carbonyl)butyl]benzamide **10**, modelled in an active site slice of the cathepsin K structure 1mem.[22,23] Proteinase residues Gln[19], Gly[23], Cys[25], Asp[61], Tyr[67], Asn[158], His[159], Trp[177] and inhibitor protons 2a, 2b, 3a, 6a are labelled for clarity.
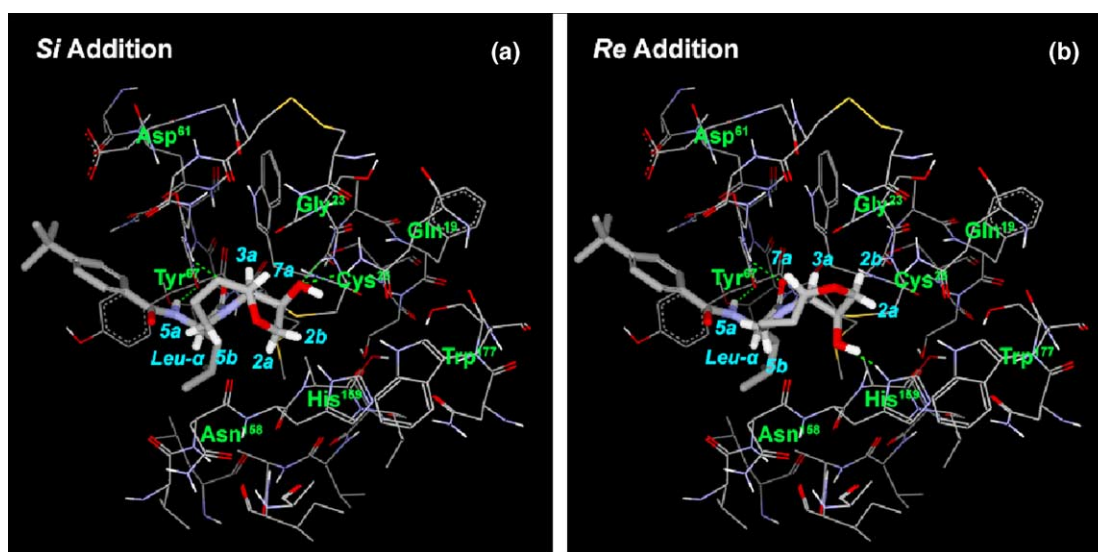

Figure 2. Predicted binding conformations for *si* (a) and *re* (b) stereofacial thiolate addition to (3aS,7aR)-4-*tert*-butyl-*N*-[3-methyl-1S-(3-oxo-hexahydro-furo[3,2-*b*]pyridine-4-carbonyl)butyl]benzamide **11**, modelled in an active site slice of the cathepsin K structure 1mem.[22,23] Proteinase residues Gln[19], Gly[23], Cys[25], Asp[61], Tyr[67], Asn[158], His[159], Trp[177] are labelled and inhibitor protons 2a, 2b, 3a, 5a, 5b, 7a and P2 Leu-α are labelled for clarity.
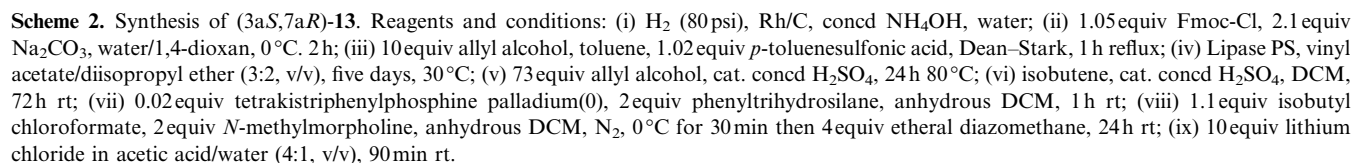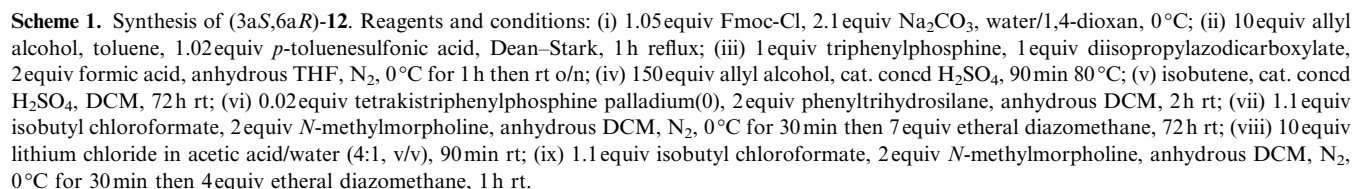
re tetrahedral adducts for the conformers shown (Fig. 2a and b). We surmised that this could have a deleterious effect on binding for analogues of **11** by inducing a rotation in the psi (Ψ) angle for the P2 leucine within the inhibitor into a sub-optimal binding conformation.

3. Chemistry

3.1. Synthesis of Fmoc protected scaffolds 12 and 13

Synthesis of compounds of general formulae **4** and **5** was envisaged through solid phase chemistry utilising the key scaffold intermediates (3aS,6aR)-3-oxo-hexa-hydrofuro[3,2-*b*]pyrrole-4-carboxylic acid 9*H*-fluoren-9-ylmethyl ester **12** and (3aS,7aR)-3-oxo-hexahydro-furo[3,2-*b*]pyridine-4-carboxylic acid 9*H*-fluoren-9-yl-methyl ester **13** (Schemes 1 and 2). Retrosynthetic analysis indicated that the adaptation of a literature method for the preparation of compounds of general formulae **1** and **2**, through a lithium chloride/acetic acid promoted insertion reaction of protected aminoacid α-diazomethylketones,[5] may provide scaffolds **12** and **13** via α-diazomethylketones **21** and **35**. It was thought that α-diazomethylketones **21** and **35** would be available from protected aminoacids **20** and **34** that in turn would be available from the free aminoacids **14** and **27**.

Scheme 1. Synthesis of (3a*S*,6a*R*)-**12**. Reagents and conditions: (i) 1.05 equiv Fmoc-Cl, 2.1 equiv Na$_2$CO$_3$, water/1,4-dioxan, 0 °C; (ii) 10 equiv allyl alcohol, toluene, 1.02 equiv *p*-toluenesulfonic acid, Dean–Stark, 1 h reflux; (iii) 1 equiv triphenylphosphine, 1 equiv diisopropylazodicarboxylate, 2 equiv formic acid, anhydrous THF, N$_2$, 0 °C for 1 h then rt o/n; (iv) 150 equiv allyl alcohol, cat. concd H$_2$SO$_4$, 90 min 80 °C; (v) isobutene, cat. concd H$_2$SO$_4$, DCM, 72 h rt; (vi) 0.02 equiv tetrakistriphenylphosphine palladium(0), 2 equiv phenyltrihydrosilane, anhydrous DCM, 2 h rt; (vii) 1.1 equiv isobutyl chloroformate, 2 equiv *N*-methylmorpholine, anhydrous DCM, N$_2$, 0 °C for 30 min then 7 equiv etheral diazomethane, 72 h rt; (viii) 10 equiv lithium chloride in acetic acid/water (4:1, v/v), 90 min rt; (ix) 1.1 equiv isobutyl chloroformate, 2 equiv *N*-methylmorpholine, anhydrous DCM, N$_2$, 0 °C for 30 min then 4 equiv etheral diazomethane, 1 h rt.

Scheme 2. Synthesis of (3a*S*,7a*R*)-**13**. Reagents and conditions: (i) H$_2$ (80 psi), Rh/C, concd NH$_4$OH, water; (ii) 1.05 equiv Fmoc-Cl, 2.1 equiv Na$_2$CO$_3$, water/1,4-dioxan, 0 °C. 2 h; (iii) 10 equiv allyl alcohol, toluene, 1.02 equiv *p*-toluenesulfonic acid, Dean–Stark, 1 h reflux; (iv) Lipase PS, vinyl acetate/diisopropyl ether (3:2, v/v), five days, 30 °C; (v) 73 equiv allyl alcohol, cat. concd H$_2$SO$_4$, 24 h 80 °C; (vi) isobutene, cat. concd H$_2$SO$_4$, DCM, 72 h rt; (vii) 0.02 equiv tetrakistriphenylphosphine palladium(0), 2 equiv phenyltrihydrosilane, anhydrous DCM, 1 h rt; (viii) 1.1 equiv isobutyl chloroformate, 2 equiv *N*-methylmorpholine, anhydrous DCM, N$_2$, 0 °C for 30 min then 4 equiv etheral diazomethane, 24 h rt; (ix) 10 equiv lithium chloride in acetic acid/water (4:1, v/v), 90 min rt.

Synthesis of building block **12** commenced from the commercially available (2*S*,3*S*)-*trans*-proline **14** in which we envisaged stereochemical inversion of the 3-hydroxyl via a suitably protected intermediate. Thus, 9-fluorenylmethoxycarbonyl (Fmoc) Nα-protection of aminoacid **14** proceeded smoothly under standard Schotten–Baumann conditions to give protected aminoacid **15** (59%). Intermediate **15** was then esterified with allyl alcohol under Dean–Stark conditions, to give Fmoc-aminoacid allyl ester (−)**16** (85%). Intermediate **16** provided a suitable analogue for application of the

Mitsunobu inversion reaction, which is well known in a host of aminoacid analogues[25] and has been described towards proline analogues functionalised at the 3-position.[26] Thus, treatment of **16** under Mitsunobu conditions in the presence of formic acid provided the C-*3* inverted formyl ester **17** (which co-eluted with the bisacylhydrazide by-product upon chromatography) along with the α,β-dehydrated product 4,5-dihydropyrrole-1,2-dicarboxylic acid 2-allyl ester 1-(9*H*-fluoren-9-yl-methyl) ester **36** (12%) and recovered **16** (35%). The formyl group was readily cleaved from intermediate **17**

5694

M. Quibell et al. / Bioorg. Med. Chem. 12 (2004) 5689–5710

by transesterification with allyl alcohol under acid catalysis to give the desired *cis*-3-hydroxyproline analogue (−)**18** (42%). Analogue **18** had not been previously described in the literature and as such a comparison of optical rotation to assign absolute stereochemical configuration was not possible. However, analysis of ^{13}C chemical shifts confirmed C-*3* hydroxyl inversion to the *cis*-isomer had occurred.[26,27] Our previous experiences had shown that the final lithium chloride promoted insertion reaction of protected aminoacid α-diazomethylketones,[5] may be performed on both the free hydroxyl and *tert*-butyl ether protected analogues, however cleaner products are generally produced via the ether route. Therefore, intermediate **18** was converted to the *tert*-butyl ether protected analogue (+)**19** (83%) by acid catalysed reaction with isobutene. Selective removal of the allyl ester following the general conditions described by Dessolin et al.[28] provided the free carboxylic acid (+)**20** (61%). In situ activation of **20** as the mixed anhydride using isobutyl chloroformate and *N*-methylmorpholine proceeded smoothly (HPLC–MS and analytical HPLC monitoring showed >95% activation). However, subsequent addition of freshly prepared etheral diazomethane to the mixed anhydride of **20** initially gave an unexplained result. One hour after addition, analysis of the reaction mixture by analytical HPLC and HPLC–MS indicated the presence of a new species with the expected MS profile for the desired bicyclic product **12** (m/z 350.2). Also present were species assigned as diazomethylketone **21** (m/z 406.2 $[M + H − N_2]^+$), the methyl ester of starting acid **20** (m/z 424.1) and the mixed anhydride (m/z 532.2 $[M + Na]^+$). The reaction mixture, which was periodically analysed as above and over the course of 72 h, suggested a smooth (although not complete) conversion of the anhydride into diazoketone **21** and *apparently* product **12**. After 72 h the reaction was quenched with acetic acid and purified to give three main fractions identified as the isobutyl mixed anhydride of acid **20**, compound **37** (20%), the methyl ester of acid **20**, compound **38** (16%) and the desired diazomethylketone **21** (24%). Re-analysis of the now purified diazomethylketone **21** solved the earlier unexpected result since **21** appeared to partially cyclise to a species that corresponded to the desired 5,5-bicycle **12** upon HPLC–MS analysis conditions. This interpretation was supported following the treatment of purified diazomethylketone **21** with lithium chloride in acetic acid/water (4:1, v/v) for 1 h, which gave a characteristic effervescence and loss of yellow colouration along with the formation of a new less mobile species on TLC. The new species was purified over silica and confirmed by full analysis as the desired 5,5-bicyclic ketone (−)**12** (79% from diazomethylketone **21** and overall 19% from acid **20**) ($[\alpha]_D^{22} − 137.2$ (*c* 0.349, CHCl$_3$)). Analytical HPLC analysis of (−)**12** gave an unusually broad elution profile, which directly contrasted the sharp peaks observed for all other intermediates along the synthetic pathway. Corresponding analysis by HPLC–MS again gave a broad profile with characteristic leading and following peak edges, which gave the expected m/z signals across the whole broad profile upon specific ion extraction. We have attributed this unusual elution behaviour to the presence under HPLC conditions of slowly converting but resolvable rotamers about the urethane 3° amide bond. Analysis of (−)**12** by ^{13}C NMR in CDCl$_3$ at room temperature also showed the presence of rotamers (coalescence upon heating to 75 °C), but a single ring-fused isomer was clearly present.

The foundations of our design process were built upon calculations, which showed *cis*-5,5-ketoheterobicycles **4** to be chirally stable, as indeed are the vast majority of the 5,5-bicycles described in the literature. However since the ketoheterobicyclic system **4** had not been experimentally described to date and in view of the surprising effects on stability of some 5,5-carbocycles upon heteroatom substitution,[16] it was important to show that the *trans*-5,5-ketoheterobicycle analogue of **4** could not be readily prepared. Therefore, we attempted preparation of a 5,5-*trans*-bicycle from *trans*-proline analogue **16**, following the general reactions detailed in Scheme 1. Intermediate (−)**16** was smoothly converted to the corresponding *tert*-butyl ether protected analogue **22** (86.0%), then to the free acid (−)**23** (40%) as generally detailed earlier. In situ activation of **23** as the mixed anhydride using isobutyl chloroformate and *N*-methylmorpholine proceeded smoothly (HPLC–MS and analytical HPLC monitoring showed >95% activation). However, subsequent addition of freshly prepared etheral diazomethane to the mixed anhydride of **23** gave essentially quantitative conversion to the corresponding diazomethylketone **24** within 1 h, which is in stark contrast to our earlier observations for the corresponding *cis*-diazomethylketone **21**. Treatment of *trans*-diazomethylketone **24** with lithium chloride in acetic acid/water (4:1, v/v) for 1 h failed to yield any hint of a bicyclic product, instead giving the α-chloromethylketone **25** (45%).[29]

Synthesis of building block **13** commenced from the commercially available 3-hydroxypicolinic acid **26**, which was hydrogenated following the literature procedure of Drummond et al.[30] to provide the starting aminoacid, 3-hydroxypipecolic acid **27** as a *cis*-racemic mixture. The enzymatic resolution of (±)-*cis*-**27** has been described by Scott and Williams[31] through the use of Lipase PS via the protected analogue (±)-*cis*-**29**. Thus, racemic aminoacid **27** was smoothly converted to Fmoc-Nα-protected analogue (±)-*cis*-**28** (79.5%) and then the corresponding allyl ester (±)-*cis*-**29** (65%) as generally detailed earlier. The *cis*-racemic **29** was then treated with Lipase PS in a mixture of vinyl acetate and isopropyl ether at 30 °C and the progress of reaction monitored by analytical HPLC and HPLC–MS. As the reaction progressed, a new product formed, which corresponded to the addition of an acetyl group to the starting material. The percentage of this new product increased over five days reaching completion where it represented 47.5% of the UV active material by HPLC compared to 52.5% residual starting material. Purification of this reaction mixture gave two products corresponding to the acetate (+)-(2*S*,3*R*)-**31** (44%) ($[\alpha]_D^{22} + 14.6$ (*c* 0.52, CHCl$_3$), lit.[31] $[\alpha]_D^{20} + 12.8$ (*c* 1.1, CH$_2$Cl$_2$)) and the alcohol (+)-(2*R*,3*S*)-**30** (46%) ($[\alpha]_D^{22} + 38.8$ (*c* 0.407, CHCl$_3$), lit.[31] $[\alpha]_D^{20} + 36.8$

(*c* 1.2, CH₂Cl₂)). The acetyl group was readily cleaved from intermediate **31** by transesterification with allyl alcohol under acid catalysis to give the desired chiral alcohol (−)-(2*S*,3*R*)-**32** (74%) ([α]$_D^{22}$ − 42.8 (*c* 0.407, CHCl₃), lit.[31] [α]$_D^{20}$ − 33.6 (*c* 1.5, CH₂Cl₂)). With chiral alcohol **32** in hand, we applied the general reasoning and chemistry detailed earlier for synthesis of building block **12** to provide building block **13**. Thus, preparation of the *tert*-butyl ether protected analogue (+)**33** (80%) was followed by removal of allyl protection to provide free acid (+)**34** (70%). In situ activation of **34** as the mixed anhydride using isobutyl chloroformate and *N*-methylmorpholine proceeded smoothly (HPLC–MS and analytical HPLC monitoring showed >95% activation). The subsequent addition of freshly prepared etheral diazomethane to the mixed anhydride of **34** gave a similar series of analyses and conclusions to those described earlier during the conversion of acid **20** to diazomethylketone **21** and bicycle **12**. One hour after addition, analysis of the reaction mixture by analytical HPLC and HPLC–MS indicated the presence of a new species with the expected MS profile for the desired bicyclic product **13** (*m/z* 364.2). Also present were species assigned as diazomethylketone **35** (*m/z* 420.2 [M + H − N₂]⁺), numerous unidentified minor species and the unreacted mixed anhydride of **34**. The reaction mixture was periodically analysed until complete consumption of the mixed anhydride was observed (24 h). Subsequent treatment of the resulting crude diazomethylketone **35** (which eluted on HPLC–MS as a species that was *apparently* the desired 6,5-bicycle **13**) with lithium chloride in acetic acid/water (4:1, v/v) for 1 h gave a characteristic effervescence and loss of yellow colouration along with the formation of a new less mobile species on TLC. The new species was purified over silica and confirmed by full analysis as the desired 6,5-bicyclic ketone (−)**13** (overall 51.9% from acid **34**) ([α]$_D^{22}$ − 13.5 (*c* 0.363, CHCl₃)).[32] Analytical HPLC analysis of bicycle (−)**13** gave a single sharp peak, which directly contrasted the broad profile described earlier for bicycle (−)**12**. Additionally, in a similar manner to bicycle

(−)**12**, analysis of (−)**13** by ¹³C NMR in CDCl₃ at room temperature showed the presence of rotamers (coalescence upon heating to 75 °C), but a single ring-fused isomer was clearly present.

3.2. Solid phase synthesis

With protected building blocks **12** and **13** in hand, we chose a solid phase synthesis to prepare appropriately functionalised analogues as potential inhibitors of CAC1 proteinases. Our synthetic strategy was based upon reversible anchorage of the ketone functionality of building blocks **12** and **13** via the hydrazide linker of Murphy et al.[33] using the general multipin techniques that we have previously described in detail (Scheme 3).[5,34]

Our earlier studies concerning α-alkylated scaffolds **1** and **2** highlighted the general increase in steric hindrance around the ketone functionality in these scaffolds as evidenced by extended linker construct formation and acidolytic cleavage times when compared to those of scaffold **3**.[5] However, when comparing kinetics for bicyclic building blocks **12** and **13**, we found that formation of linker constructs **43a** and **44a** occurred within 2 h indicating that the ketone functionality within these scaffolds was readily accessible. Additionally, the efficiency of acidolytic cleavage from the solid phase was dramatically improved when compared to that of the α-alkylated scaffolds **1** and **2**. We were encouraged by these simple reaction time observations since they indicated that the bi-cyclisation approach to chiral stability described herein may additionally provide a ketone functionality that was free from the steric hindrance observed in the alternative α-alkylation approach previously described.[5] Final compounds **10**, **45a–e** and **11**, **46** were prepared from linker constructs **43b** and **44b** by a series of sequential washing and coupling reaction steps involving removal of Fmoc, coupling of an activated Fmoc-NHCHR²-COOH, removal of Fmoc, coupling of an activated R³-COOH, acidolytic cleavage
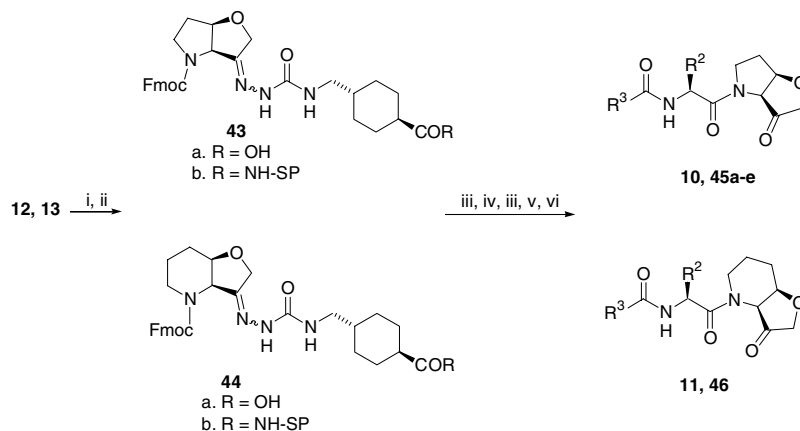
Scheme 3. Synthesis and use of supported linker constructs **43b** and **44b** towards full length inhibitors **10**, **45a–e** and **11**, **46**. Reagents and conditions: (i) *trans*-4{[(hydrazino carbonyl)amino]methyl}cyclohexanecarboxylic acid, trifluoroacetate, EtOH, H₂O, NaOAc, reflux; (ii) 3 equiv **43a** or **44a**, 3 equiv HBTU, 3 equiv HOBt, 6 equiv NMM, H₂N-solid phase, DMF; (iii) 20% piperidine/DMF (v/v), 30 min; (iv) 20 equiv Fmoc-NHCHR²-COOH, 20 equiv HBTU, 20 equiv HOBt, 40 equiv NMM, DMF, rt, o/n, then repeat with fresh reagents for 6 h; (v) 10 equiv R³-COOH, 10 equiv HBTU, 10 equiv HOBt, 20 equiv NMM, DMF, rt o/n; (vi) TFA/H₂O, (95:5, v/v), 2 h.

and semi-preparative HPLC purification.[35] The coupling of activated Fmoc-aminoacids to the free secondary amine functionality of the solid phase bound bicyclic scaffolds **43b** and **44b** was found to be somewhat hindered and required an extended double coupling protocol to reach completion.
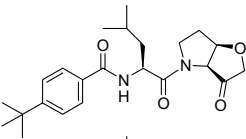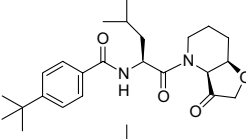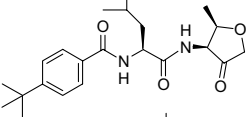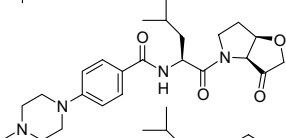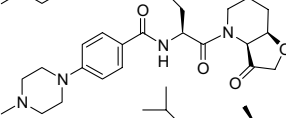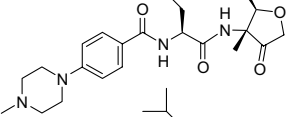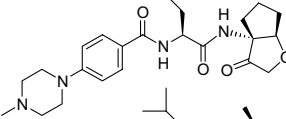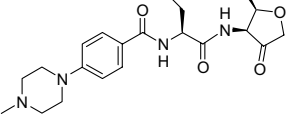
3.3. Enzyme inhibition studies

Bicyclic inhibitors **10**, **45a–e** and **11**, **46** were prepared, purified and then screened against cathepsins B, K, L and S as well as the parasitic proteinases cruzain and CPB.[8a,b] The preliminary steady-state inhibition constants (K_i^{ss}) are shown in Table 1 (mean of $n = 3$ determinations). The substituents detailed in Table 1 were chosen to exemplify binding groups that provide potent inhibitors when combined with the unsubstituted monocyclic scaffold **3**.

Table 1 clearly shows that the bi-cyclisation rationale and design process described herein provides potent

and selective inhibitors of human cathepsin K. In particular, the 5,5-bicyclic analogues **10** and **45a** exhibit similar or improved potency when compared to the parent monocyclic analogues **49a** and **49b**, in combination with a generally improved selectivity profile against other CAC1 proteinases. However, when the 5,5-bicycle was ring-expanded to the 6,5-bicyclic analogues **11** and **46**, we observed an approximately 85 and 135-fold loss in potency, respectively. These experimental observations are consistent with our conclusions drawn earlier upon examination of the binding conformations depicted in Figures 1a,b and 2a,b. Here, it appears that the extra methylene present in the 6,5-system may induce a suboptimal binding conformation for the inhibitor P2 leucine moiety.[37]

Based upon the exciting results observed for the inhibition of human cathepsin K with 5,5-bicyclic analogues **10** and **45a**, we designed a further series of analogues to ascertain whether the bi-cyclisation process was applicable towards other CAC1 proteinases. Therefore ana-

Table 1. Preliminary inhibitory activities (K_i^{ss}, nM) for 5,5-(**10**, **45a**) and 6,5-(**11**, **46**) bicyclic inhibitors against CAC1 proteinases (mean of $n = 3$ determinations)

No.	Structure	Cat. K	Cat. L	Cat. S	Cat. B	Cruz.	CPB
10		87.4 ± 0.8	>25,000	>41,000	NI	2044 ± 267	2529 ± 153
11		7000 ± 594	>44,000	>85,000	NI	NI	>59,000
49a (Ref. 36)		41.0 ± 2.1	5849 ± 1925	>29,000	NI	912 ± 114	1191 ± 226
45a		8.7 ± 0.4	>10,000	>40,000	NI	2901 ± 289	813 ± 107
46		1169 ± 73	>39,000	NI	NI	>95,000	>44,000
47 (Ref. 5)		8700 ± 1100	>65,000	NI	NI	NI	>50,000
48 (Ref. 5)		1800 ± 200	21,000	>40,000	NI	12,300	21,000
49b (Ref. 36)		38.9 ± 2.7	1266 ± 275	>14,000	NI	1717 ± 106	497 ± 64

Various α-alkylated[5] and monocyclic standards[36] are included for comparison. NI denotes no observed inhibition.

logues **45b**–**e** were prepared and assayed for inhibitory activity[8a,b] and compared to the corresponding monocyclic analogues.[36] The results clearly showed that our bicycles had wider applicability. For example, analogue **45b** was a potent ($K_i^{ss} = 650\,nM$) and selective (>10-fold vs K and L) inhibitor of bovine cathepsin S with potency approaching that of the parent monocycle standard ($K_i^{ss} = 220\,nM$) and a significant improvement in potency when compared to the corresponding α-alkylated analogues.[5] Analogue **45c** was a selective 1.9 µM inhibitor of cathepsin L, however this represented a 25-fold loss in potency when compared to the corresponding parent monocyclic inhibitor ($K_i^{ss} = 70\,nM$); analogue **45d** was a mixed (but selective vs S, L and B) inhibitor of cathepsin K ($K_i^{ss} = 325$ nM) and CPB ($K_i^{ss} = 540\,nM$) with potency virtually identical to the corresponding parent monocyclic inhibitor; analogue **45e** was a selective 1.3 µM inhibitor of cruzain, which represented only a threefold loss in potency when compared to the corresponding parent monocyclic inhibitor ($K_i^{ss} = 400\,nM$).
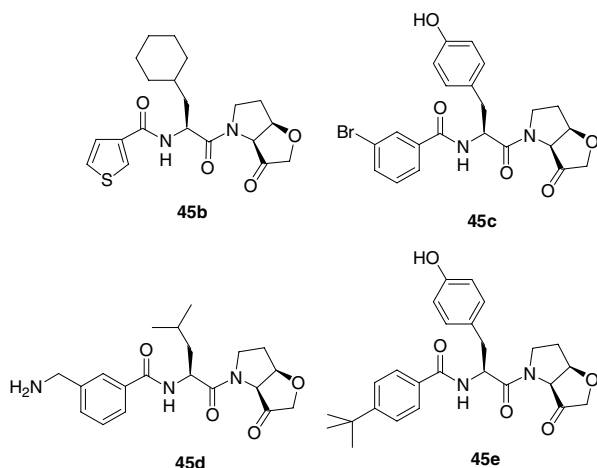
In order to gain a better understanding for the dramatic difference in potency when comparing the 5,5- and 6,5-bicyclic inhibitors, individual association (k_{on}) and dissociation (k_{off}) rate constants were determined for **10**, **45a** and **11**, **46** against human cathepsin K. These results were compared to our previously described α-alkylated analogues[5] and the parent monocyclic inhibitors[36] and are shown in Table 2. It was clear that the 5,5-bicyclic analogues **10** and **45a** exhibited association and dissoci-

ation rates broadly similar to those of the parent monocycles **49a** and **49b** and hence are equipotent. However, in a similar manner to that observed for the α-alkylated analogues **47** and **48**, the 6,5-bicycles **11** and **46** exhibit a dramatic drop in the association rate, which results in the loss of potency.

3.4. In vitro stability and physiochemical properties

Having established that the bicycles led to potent and selective inhibitors of CAC1 proteinases, we further evaluated analogues **10**, **45a** and for comparison **11**, **46** through a range of stability studies, physiochemical property determinations and in vitro secondary assays (Tables 3 and 4). These studies aimed to establish the basic physical properties exhibited by our novel bicyclic analogues and to determine their suitability for functional assessment of cathepsin K inhibition.[38] All four analogues exhibited good stability at neutral pH and analogues **45a** and **46** also exhibited good stability under basic conditions. However under acidic conditions, the 5,5-bicycle analogues **10** and **45a** were significantly more stable than the corresponding 6,5-bicycles **11** and **46**. In each case, the loss of parent compound was accompanied by appearance of the carboxylic acid that derives from cleavage of the 3° amide bond. Additionally during these HPLC analyses, the parent peak shape of each of the four analogues was closely monitored, particularly during the base stability assays where formation of the enol intermediate may be promoted leading to loss of α-chirality.[6b] In each case the parent peak shape remained unchanged with no evidence of the diastereomeric *trans* bicycle that would result through epimerisation of the α-chiral centre.[39] These findings are in agreement with our conformational energy calculations that predicted that 5,5-bicycles such as compounds **10** and **45a** should exhibit α-chiral stability because the *cis*-fused geometry is of a substantially lower steric energy than that of the corresponding *trans*-fused geometry.[12] Our findings also indicate that 6,5-bicycles such as compounds **11** and **46** show chiral stability under the conditions examined, even though the parent 6,5-ketocarbocycles are known in both *cis*[13d] and *trans*[13b] conformations. Here, the addition of heteroatoms and the bulky substituted nitrogen to the parent 6,5-ketocarbocycle appears to give a system where either the *cis*-fused geometry is significantly more stable than the corresponding *trans* and/or the energy barrier for enolisation is large.

Table 2. Association (k_{on}) and dissociation rate constants (k_{off}) for selected inhibitors against human cathepsin K[7]

No.	k_{on} (M^{-1}s^{-1}) ($\times 10^5$)	k_{off} (s^{-1}) ($\times 10^{-3}$)	K_i k_{off}/k_{on}[a] (M) ($\times 10^{-9}$)
10	4.9 ± 3.9	7.5 ± 1.7	15.2
11	0.0031 ± 0.0018	11.7 ± 6.0	37,900
49a (Ref. 36)	12.0 ± 2.0	40.3 ± 21.5	33.6
45a	5.3 ± 4.6	5.5 ± 0.7	10.4
46	0.0121 ± 0.0020	36.3 ± 29.6	30,000
47 (Ref. 5)	0.0036 ± 0.0001	8.1 ± 1.0	22,800
48 (Ref. 5)	0.0063 ± 0.0036	22.6 ± 3.8	35,900
49b (Ref. 36)	>10	18.7 ± 14.6	—

[a] The corresponding steady-state inhibition constants (K_i^{ss}) are shown in Table 1.

Table 3. Stability studies for bicyclic analogues **10**, **45a** and **11**, **46**

No.	PBS (pH 7.4) $t_{1/2}$ (h)[a]	Acid ($\sim$pH 1.5) $t_{1/2}$ (h)[b]	Base (pH 10.5) $t_{1/2}$ (h)[c]	Human plasma $t_{1/2}$ (h)[d]	HLM $t_{1/2}$ (h)[e]
10	28.9	23.2	n.d.	4.5	2.8
45a	36.5	16.9	27.9	16.3	7.5
11	47.4	0.9	n.d.	37.8	0.3
46	49.9	1.1	48.4	34.1	1.7

For each analysis, aliquots at appropriate times were quantified by HPLC–MS, using single ion monitoring and the ion intensity data converted to a $t_{1/2}$ for loss of parent analogue.

[a] Compounds were incubated at 10 μM in PBS (10 mM; pH 7.4) at 37 °C.
[b] Compounds were incubated at 10 μM in 0.1 M HCl/acetonitrile (80:20) at 37 °C.
[c] Compounds were incubated at 10 μM in potassium phosphate (10 mM; pH 10.5) at 37 °C.
[d] Compounds were incubated at 10 μM in human plasma at 37 °C and after protein precipitation with acetonitrile, extracted aliquots were analysed by HPLC–MS, using single ion monitoring.
[e] Compounds were incubated at 50 μM with human liver microsomes (0.5 mg/mL of microsomal protein, final concentration) in potassium phosphate (50 mM; pH 7.4) at 37 °C and the reaction was initiated with NADPH (1 mM final concentration). Quenching was achieved by protein precipitation with acetonitrile and the extracted aliquots were analysed by HPLC, employing UV detection.

Table 4. Physiochemical properties for bicyclic analogues **10**, **45a** and **11**, **46**

No.	Sol.[a]	Log $D_{7.4}$[b]	No. H-bond donors	No. H-bond acceptors	No. rotatable bonds	Polar surface area (Å^2)
10	M	1.36	1	4	6	75.7
45a	H	0.04	1	6	6	82.2
11	L	2.99	1	4	6	75.7
46	H	0.85	1	6	6	82.2

[a] Aqueous solubility was assessed by measuring turbidity of solutions of compound prepared in PBS (10 mM; pH 7.4) at 200, 100, 50 and 25 μM, by light scattering at 650 nm. Compounds were assigned as having high (H, >100 μM), medium (M, 50–100 μM) or low (L, <50 μM) solubility.
[b] Partitioning of the compounds between *n*-octanol and PBS (10 mM; pH 7.4) was assessed using a miniaturised shake-flask method, employing HPLC-UV analysis.

The stability of analogues **10**, **45a** and **11**, **46** was also assessed in human plasma and a human liver microsome (HLM) preparation (which contains the major phase I metabolising enzymes) as a prelude to their potential use in cell-based assays. At this stage we were primarily concerned with quantifying loss of parent peak rather than stringent identification of metabolites and the results are presented in Table 3. In human plasma, the 6,5-analogues **11** and **46** were significantly more stable than the corresponding 5,5-analogues **10** and **45a**, whilst in an HLM preparation the opposite trend was observed with the 5,5-bicycles exhibiting significantly more stability than the corresponding more lipophilic 6,5-bicycles. Additionally, the HLM assay showed the more lipophilic *tert*-butyl analogues (**10** and **11**) to be significantly less stable than the corresponding *N*-methylpiperazinyl analogues (**45a** and **46**).

The basic physiochemical properties of analogues **10**, **45a** and **11**, **46** are presented in Table 4. All four analogues have molecular properties that conform to major predictors of desirable drug-like features with a moderate number of hydrogen bond donors and acceptors,[40] medium polar surface area,[24] moderate molecular weight (401–457 Da) and moderate rotational freedom.[24]

Finally, we assessed selected 5,5 and 6,5-bicyclic analogues in a series of secondary in vitro and cell-based assays. As a prediction of potential drug–drug interactions, analogues **10**, **45a** and **11**, **46** were assessed in vitro against the major cytochrome P450 isozymes 1A2, 2B6, 2D6, 3A4 and 2C19 showing no significant inhibition at 10 μM.[41] Analogue **10** was further assessed for Caco-2 membrane permeability (TC7 sub-clone, pH 6.5 in A and 7.4 in B) giving apical-to-basolateral permeability at 12.5×10^{-6} cm/s (0.045 cm/h) and basolateral-to-apical at 24.3×10^{-6} cm/s (0.087 cm/h). Analogue **10** was also assessed for cytotoxicity in both human and rat primary hepatocytes showing no adverse effects at the test concentration of 30 μM. Considering these findings and the results from Tables 3 and 4, we concluded that analogue **10** exhibited a reasonably good range of properties suitable for functional assessment of cathepsin K inhibition.

3.5. Osteoclast resorption assay

To address the general ability of our bicyclic cathepsin K inhibitors to inhibit bone resorption, analogue **10** was evaluated in a human osteoclast resorption assay.[42] Briefly, human osteoclasts were cultured on bovine bone slices and allowed to differentiate and resorb bone, thus releasing C-terminal telopeptides (CTX) of type I collagen into the culture media, which are quantified as an index of bone resorption. Compound **10** and a positive control, E-64 (a potent inhibitor of cathepsin K), were added into the cell cultures after the differentiation period and their effects on the resorbing activity of mature osteoclasts were determined (Fig. 3). As shown in Figure 3, compound **10** inhibits bone resorption in a dose-dependant manner with an IC$_{50}$ between 0.1 and 1.0 μM.
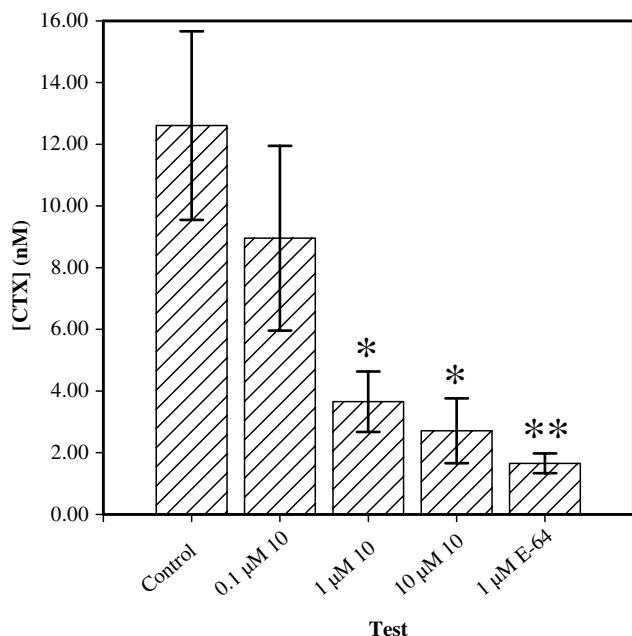
Figure 3. Inhibition profile for compound **10** as judged by human osteoclast bone resorption assay. Bone resorption activity was monitored by determining collagen fragments in culture medium (CTX) using CrossLaps®. Asterisks indicate values that are statistically significantly different from baseline (with a *p*-value of less than 0.05). One asterisk (*) indicates a *p*-value between 0.05 and 0.01 and two asterisks (**) a *p*-value between 0.01 and 0.001.

4. Conclusions

We have designed a 5,5-bicyclic ketone containing scaffold that is chirally stable due to the marked energetic preference for a *cis*-fused compared to *trans*-fused geometry. This chiral stability provides a major advance when compared to monocyclic ketones that often show limited potential for pre-clinical development due to chiral instability. Additionally, our 5,5-scaffold provides the first disclosure of a conformationally constrained design that exhibits potent inhibition of CAC1 proteinases. We believe that the many potential advantages provided by constraint into a bicyclic scaffold have not been exploited to date for CAC1 proteinase inhibition primarily because the P1 NH moiety present in all other substrate-based inhibitor series has been perceived as essential for low nanomolar potency. Our 5,5-scaffold now provides the first departure from this previously accepted paradigm. The ring-expanded 6,5-bicyclic scaffold designed considering the same basic principles also shows chiral stability. However, the 6,5-bicycle provided analogues that were considerably less potent in vitro than the corresponding 5,5-bicycle analogues. Upon rigorous kinetic analysis of potent cathepsin K inhibitor analogues derived from the 5,5- and 6,5-scaffolds, it was clear that the 5,5-analogues are potent due to an association rate with the proteinase that is similar to the corresponding monocyclic ketones, whereas the 6,5-analogues have a significantly slower association rate and hence a subsequent loss in potency. A representative cathepsin K inhibitor designed around

the 5,5-bicycle, compound **10**, exhibited a reasonably good range of physiochemical and stability properties in both chemical and biological media and was assessed in a human osteoclast functional assay of cathepsin K inhibition. Compound **10** exhibited sub-micromolar potency in this cell-based assay, offering the potential for development of more potent analogues from this series towards a cathepsin K inhibitor for the treatment of osteoporosis.

5. Experimental

5.1. General procedures

Standard vacuum techniques were used in handling of air sensitive materials. Solvents were purchased from ROMIL Ltd, U.K. at SpS or Hi-Dry grade unless otherwise stated. Lipase PS was purchased from Amano Enzyme Europe Ltd. ^{1}H NMR and ^{13}C NMR were obtained on a Bruker DPX400 (400 MHz ^{1}H frequency and 100 MHz ^{13}C frequency; QXI probe) in the solvents indicated. Chemical shifts are expressed in parts per million (δ) and are referenced to residual signals of the solvent. Coupling constants (J) are expressed in Hz. All analytical HPLC were obtained on Phenomenex Jupiter C$_4$, 5 μm, 300 Å, 250 × 4.6 mm, using mixtures of solvent A = 0.1% aq trifluoroacetic acid (TFA) and solvent B = 90% acetonitrile/10% solvent A on automated Agilent systems with 215 and/or 254 nm UV detection. Unless otherwise stated a gradient of 10–90% B in A over 25 min at 1.5 mL/min was performed for full analytical HPLC. HPLC–MS analysis was performed on an Agilent 1100 series LC/MSD, using automated Agilent HPLC systems, with a gradient of 10–90% B in A over 10 min on Phenomenex Luna C$_8$, 5 μm, 300 Å, 50 × 2.0 mm at 0.6 mL/min. Semi-preparative HPLC purification was performed on Phenomenex Jupiter C$_4$, 5 μm, 300 Å, 250 × 10 mm, using a gradient of 10–90% B in A over 25 min at 4 mL/min on automated Agilent systems with 215 and/or 254 nm UV detection. Flash column purification was performed on silica gel 60 (Merck 9385). Polyamide multipins (10 μmol loadings, SPMDINOF, see http://www.mimotopes.com) were used for the solid phase synthesis. Biochemical protocols together with enzyme assays were carried out as previously described.[8a,b] Substrates utilizing fluorescence resonance energy transfer methodology (i.e., FRET-based substrates) were synthesised using standard solid phase Fmoc chemistry methods,[43] and employed Abz (2-aminobenzoyl) as the fluorescence donor and 3-nitrotyrosine [Tyr(NO$_2$)] as the fluorescence quencher.[44]

5.2. (2*S*,3*S*)-(3-Hydroxy)pyrrolidine-1,2-dicarboxylic acid 1-(9*H*-fluoren-9-ylmethyl) ester (15)

trans-3-Hydroxy-L-proline (**14**) (10.0 g, 76.3 mmol) was added to a vigorously stirred, ice-cooled solution of sodium carbonate (16.90 g, 160.2 mmol) in water (100 mL). 1,4-Dioxan (75 mL) was added providing an opaque but mobile mixture. 9-Fluorenylmethyl chloroformate (20.31 g, 80 mmol) in 1,4-dioxan (75 mL) was

added over 1 h, then the ice-cooling removed and the mixture stirred at ambient temperature for an additional 2 h. Additional water (300 mL) was added, the reaction mixture washed with chloroform (2×250 mL) and the combined organic layers discarded. The aqueous phase was acidified with 1 N HCl to ~pH 2, providing a thick opaque mixture. The acidified aqueous mixture was extracted with chloroform (2×500 mL) and the now clear aqueous phase discarded. The opaque combined chloroform layers were dried (Na_2SO_4), filtered and reduced in vacuo to provide batch 1 (5.70 g). The residual precipitate (a mixture of product and drying agent) was triturated with hot methanol (2×250 mL) and the combined methanol solutions reduced in vacuo to provide batch 2 (10.25 g). Batches 1 and 2 were individually analysed by TLC (single UV spot, $R_f = 0.15$, 20% MeOH in CHCl$_3$), and HPLC–MS (single main UV peak with $t_R = 7.1$ min, 354.2 $[M + H]^+$, 376.2 $[M + Na]^+$) and found to be identical and combined (15.95 g, 59%). Analysis by ^{1}H and ^{13}C NMR showed the presence of rotamers around the 3° amide bond. ^{1}H NMR (400 MHz, DMSO-d_6 at 298 K): δ 1.80–2.02 (m, NCH$_2$CH$_2$, 2H), 3.49–3.62 (m, NCH$_2$CH$_2$, 2H), 4.12–4.38 (m, CH$_\alpha$, CH$_\beta$, Fmoc H-9 and CH$_2$, 5H), 5.55/5.62 (br s, OH), 7.30–7.31 (Fmoc H-2 and H-7, 2H), 7.35–7.37 (Fmoc H-3 and H-6, 2H), 7.43–7.45 (Fmoc H-1 and H-8, 2H), 7.63–7.65 (Fmoc H-4 and H-5, 2H), 12.8–13.0 (COOH); ^{13}C NMR (100 MHz, DMSO-d_6 at 298 K): δ 31.70/32.70 (NCH$_2$CH$_2$), 44.68/45.32 (NC$_2$CH$_2$), 46.94/46.97 (Fmoc C-9), 67.04/67.33 (Fmoc CH$_2$), 68.24/68.51 (C$_\alpha$), 73.12/74.23 (C$_\beta$), 120.49/120.52 (Fmoc C-4 and C-5), 125.49/125.58 (Fmoc C-1 and C-8), 127.50 (Fmoc C-2 and C-7), 128.04 (Fmoc C-3 and C-6), 140.99/141.09 (Fmoc C-4′ and C-5′), 144.02/144.16 (Fmoc C-1′ and C-8′), 154.33/154.54 (OCON), 172.10/172.39 (COOH).

5.3. (−)-(2S,3S)-(3-Hydroxy)pyrrolidine-1,2-dicarboxylic acid 2-allyl ester 1-(9H-fluoren-9-ylmethyl) ester (16)

Compound 15 (10.9 g, 30.8 mmol) was dissolved in toluene (75 mL) in a Dean–Stark apparatus. Allyl alcohol (20 mL) was added followed by p-toluenesulfonic acid hydrate (6.05 g, 31.4 mmol). The mixture was refluxed for 1 h, cooled and CHCl$_3$ (300 mL) added. The organic layer was washed with NaHCO$_3$ (300 mL), 0.1 N HCl (300 mL) and brine (300 mL), then dried (Na$_2$SO$_4$). Filtration and reduction in vacuo gave a pale yellow foam (13.5 g). The crude foam was purified over silica gel (150 g) eluting with a gradient of heptane–ethyl acetate $3:1 \rightarrow 1:1$. Desired fractions were combined and reduced in vacuo to a colourless oil (10.34 g, 85%). TLC (single UV spot, $R_f = 0.30$, heptane–ethyl acetate 1:1), analytical HPLC $t_R = 18.8$ min, HPLC–MS (single main UV peak with $t_R = 8.4$ min, 394.2 $[M + H]^+$, 416.2 $[M + Na]^+$). Microanalysis indicated the presence of residual solvent following drying in vacuo and re-drying at elevated temperature lead to partial thermal decomposition. Exact mass calcd for C$_{23}$H$_{23}$NO$_5$ (MNa$^+$): 416.1468, found 416.1480 (δ 2.87 ppm); $[\alpha]_D^{22} - 30.5$ (c 0.282, CHCl$_3$). Analysis by ^{1}H and ^{13}C NMR showed the presence of rotamers around the 3° amide bond. ^{1}H NMR (400 MHz, CDCl$_3$ at 298 K): δ 2.00–2.21 (m,

NCH$_2$CH$_2$, 2H), 2.70/2.85 (b, OH), 3.72–3.81 (m, NCH$_2$CH$_2$, 2H), 4.12–4.67 (m, CH$_\alpha$, CH$_\beta$, Fmoc H-9 and CH$_2$, OCH$_2$CH=CH$_2$, 7H), 5.20–5.40 (m COOCH$_2$CH=CH$_2$, 2H), 5.82–5.99 (m, OCH$_2$CH=CH$_2$, 1H), 7.28–7.33 (Fmoc H-2 and H-7, 2H), 7.34–7.41 (Fmoc H-3 and H-6, 2H), 7.53–7.66 (Fmoc H-1 and H-8, 2H), 7.77–7.81 (Fmoc H-4 and H-5, 2H); ^{13}C NMR (100 MHz, CDCl$_3$ at 298 K): δ 32.28/33.04 (NCH$_2$CH$_2$), 44.98/45.32 (NCH$_2$CH$_2$), 47.56/47.63 (Fmoc C-9), 66.44 (OCH$_2$CH=CH$_2$), 68.01/68.11 (Fmoc C$_2$), 68.32/68.72 (C$_\alpha$), 74.49/75.67 (C$_\beta$), 119.20/119.48 (OCH$_2$CH=CH$_2$), 120.34/120.37 (Fmoc C-4 and C-5), 125.36/125.60 (Fmoc C-1 and C-8), 127.47 (Fmoc C-2 and C-7), 128.06/128.12 (Fmoc C-3 and C-6), 131.79/131.94 (OCH$_2$CH=CH$_2$), 141.65/141.71 (Fmoc C-4′ and C-5′), 144.12/144.34 (Fmoc C-1′ and C-8′), 155.13/155.59 (OCON), 170.53/170.55 (COOCH$_2$CH=CH$_2$).

5.4. (2S,3R)-3-Formyloxy-pyrrolidine-1,2-dicarboxylic acid 2-allyl ester 1-(9H-fluoren-9-ylmethyl) ester (17)

Triphenylphosphine (2.76 g, 10.5 mmol) was dissolved in anhydrous tetrahydrofuran (75 mL), under a nitrogen blanket with stirring and ice-cooled. Diisopropylazodicarboxylate (2.12 g, 2.07 mL, 10.5 mmol) was added dropwise over 15 min to give a white precipitous mixture. Compound 16 (4.15 g, 10.5 mmol) and formic acid (0.97 g, 0.79 mL, 21.0 mmol) were mixed in anhydrous tetrahydrofuran (30 mL) and added over 15 min to the above reaction mixture. The reaction was stirred for a further 1 h at 0 °C, then overnight at ambient temperature. The solvents were removed in vacuo to give a viscous pale yellow oil (11.1 g). The crude oil was purified over silica gel (250 g) eluting with a gradient of heptane–ethyl acetate $4:1 \rightarrow 1:1$. Product fractions were identified and reduced in vacuo to give a mixture of 17 and bis-acylhydrazide, a white solid, yield 4.0 g. TLC (single UV spot, $R_f = 0.50$, heptane–ethyl acetate 1:1), analytical HPLC $t_R = 19.1$ min, HPLC–MS (single main UV peak with $t_R = 9.7$ min, 422.2 $[M + H]^+$, 444.1 $[M + Na]^+$ and a non-UV peak with $t_R = 5.0$ min, 205.1 $[M + H]^+$, 431.2 $[2M + Na]^+$). Crude 17 was used directly in the following reaction.

Also isolated were recovered starting material 16 (1.45 g), TLC (single UV spot, $R_f = 0.30$, heptane–ethyl acetate 1:1), HPLC–MS (single main UV peak with $t_R = 8.8$ min, 394.2 $[M + H]^+$, 416.2 $[M + Na]^+$); 4,5-dihydropyrrole-1,2-dicarboxylic acid 2-allyl ester 1-(9H-fluoren-9-ylmethyl) ester (36) (0.49 g), TLC (single UV spot, $R_f = 0.65$, heptane–ethyl acetate 1:1), analytical HPLC $t_R = 20.8$ min, HPLC–MS (single main UV peak with $t_R = 10.1$ min, 376.1 $[M + H]^+$, 398.1 $[M + Na]^+$).

5.5. (−)-(2S,3R)-(3-Hydroxy)pyrrolidine-1,2-dicarboxylic acid 2-allyl ester 1-(9H-fluoren-9-ylmethyl) ester (18)

Crude compound 17 (4.0 g) was dissolved in allyl alcohol (18 mL), concd H$_2$SO$_4$ (75 μL) added and the mixture heated to reflux for 90 min. The mixture was cooled, EtOAc (200 mL) added and washed with NaHCO$_3$

(200 mL), brine (200 mL) and dried (Na_2SO_4). The solvents were removed in vacuo to give a viscous tan oil (4.2 g). The crude oil was purified over silica gel (150 g) eluting with a gradient of heptane–ethyl acetate 2:1 → 1:1. Desired fractions were combined and reduced in vacuo to a colourless gum (1.75 g, 42%). TLC (single UV spot, R_f = 0.25, heptane–ethyl acetate 1:1), analytical HPLC t_R = 17.8 min, HPLC–MS (single main UV peak with t_R = 8.6 min, 394.2 $[M + H]^+$, 416.2 $[M + Na]^+$). Anal. Calcd for $C_{23}H_{23}NO_5$: C, 70.21; H, 5.89; N, 3.56. Found: C, 69.83; H, 5.82; N, 3.49. Exact mass calcd for $C_{23}H_{23}NO_5$ (MH^+): 394.1649, found 394.1652 (δ +0.65 ppm); $[\alpha]_D^{22}$ − 40.0 (c 0.678, $CHCl_3$). Analysis by ^1H and ^{13}C NMR showed the presence of rotamers around the 3° amide bond. ^1H NMR (400 MHz, $CDCl_3$ at 298 K): δ 2.09–2.19 (m, $NCH_2CH_2$2H), 2.52 (dd, J = 4.00 Hz, OH), 3.54–3.65/ 3.70–3.82 (m, NCH_2CH_2, 2H), 4.14–4.20/4.22–4.30 (m, Fmoc H-*9*), 4.30–4.39 (m, Fmoc CH_2, 1H), 4.43–4.58 (m, CH_α + Fmoc CH_2, 2H), 4.60–4.65 (CH_β, 1H), 4.65–4.76 (m, OCH_2CH=CH_2, 2H), 5.23–5.36 (m, COOCH$_2$CH=C$H_2$2H), 5.81–6.00 (m, OCH$_2$CH=CH$_2$, 1H), 7.28–7.38 (Fmoc H-*2* and H-*7*, 2H), 7.39–7.46 (Fmoc H-*3* and H-*6*, 2H), 7.53–7.69 (Fmoc H-*1* and H-*8*, 2H), 7.73–7.81 (Fmoc H-*4* and H-*5*, 2H); ^{13}C NMR (100 MHz, $CDCl_3$ at 298 K): δ 32.34/33.22 (NCH_2CH_2), 44.65/44.90 (NCH_2CH_2), 47.57/47.63 (Fmoc C-*9*), 63.89/64.22 (C_α), 66.38/66.41 (OCH_2-CH=CH$_2$), 68.02 (Fmoc CH_2), 71.84/72.80 (C_β), 119.08/119.31 (OCH$_2$CH=CH_2), 120.39 (Fmoc C-*4* and C-*5*), 125.32/125.46/125.56 (Fmoc C-*1* and C-*8*), 127.46 (Fmoc C-*2* and C-*7*), 128.12 (Fmoc C-*3* and C-*6*), 132.03/132.14 (OCH$_2$$CH$=CH$_2$), 141.65/141.69 (Fmoc C-*4′* and C-*5′*), 144.00/144.16/144.43/144.48 (Fmoc C-*1′* and C-*8′*), 154.88/155.25 (OCON), 169.94/ 169.99 (COOCH$_2$CH=CH$_2$).

5.6. (+)-(2*S*,3*R*)-3-*tert*-Butoxy-pyrrolidine-1,2-dicarboxylic acid 2-allyl ester 1-(9*H*-fluoren-9-ylmethyl) ester (19)

Compound **18** (1.75 g, 4.45 mmol) was dissolved in anhydrous dichloromethane (20 mL) in a 50 mL glass pressure tube and cooled to −78 °C. Isobutylene (∼10 mL) was condensed into the solution and concd H_2SO_4 (100 μL) added. The tube was sealed and stirred at ambient temperature for 72 h. The sealed tube was cooled to −78 °C, *N*-methylmorpholine (200 μL, 1 equiv w.r.t. concd H_2SO_4) added and allowed to warm to ambient temperature, unsealed, with stirring over 2 h. Dichloromethane (75 mL) was added and the organics washed with $NaHCO_3$ (75 mL), then brine (75 mL) and dried (Na_2SO_4). The solvents were removed in vacuo to give a mobile pale tan oil (2.41 g). The crude oil was purified over silica gel (150 g) eluting with a gradient of heptane–ethyl acetate 4:1 → 3:1. Desired fractions were combined and reduced in vacuo to a thick clear oil (1.66 g, 83%). TLC (single UV spot, R_f = 0.45, heptane–ethyl acetate 2:1), analytical HPLC t_R = 22.8 min, HPLC–MS (single main UV peak with t_R = 11.2 min, 450.2 $[M + H]^+$, 472.2 $[M + Na]^+$, 921.4 $[2M + Na]^+$); $[\alpha]_D^{22}$ + 26.2 (c 0.168, $CHCl_3$).

5.7. (+)-(2*S*,3*R*)-3-*tert*-Butoxy-pyrrolidine-1,2-dicarboxylic acid 1-(9*H*-fluoren-9-ylmethyl) ester (20)

Compound **19** (1.60 g, 3.56 mmol) was dissolved in anhydrous dichloromethane (20 mL) with stirring. Tetrakistriphenylphosphine palladium(0) (83 mg, 0.071 mmol, 0.02 equiv) was added, followed by phenyltrihydrosilane (0.77 g, 0.674 mL, 7.12 mmol, 2 equiv). After 2 h, dichloromethane (150 mL) was added and the organics washed with 0.01 N HCl (150 mL), brine (150 mL) and dried (Na_2SO_4). The solvents were removed in vacuo to give a dark grey solid (2.14 g). The crude solid was purified over silica gel (75 g) eluting with a gradient of heptane–ethyl acetate 2:1 → 1:6. Desired fractions were combined and reduced in vacuo to a white crystalline solid (0.89 g, 61%). TLC (single UV spot, R_f = 0.30, heptane–ethyl acetate 1:2), analytical HPLC t_R = 19.1 min, HPLC–MS (single main UV peak with t_R = 9.4 min, 354.1 $[M + H - Bu^t]^+$, 410.2 $[M + H]^+$, 432.1 $[M + Na]^+$, 841.1 $[2M + Na]^+$). Microanalysis indicated the presence of residual solvent following drying in vacuo and re-drying at elevated temperature lead to partial thermal decomposition. Exact mass calcd for $C_{24}H_{27}NO_5$ (MH^+): 410.1962, found 410.1960 (δ 0.52 ppm); $[\alpha]_D^{22}$ + 12.2 (c 0.409, $CHCl_3$). Analysis by ^1H and ^{13}C NMR showed the presence of rotamers around the 3° amide bond. ^1H NMR (400 MHz, $CDCl_3$ at 298 K): δ 1.23 (s, C(CH_3)$_3$, 9H), 1.98–2.28 (m, NCH$_2$CH_2, 2H), 3.40–3.50 (m, NCH_2CH$_2$, 1H), 3.68–3.81 (m, NCH_2CH$_2$, 1H), 4.10–4.50 (m, CH_α + CH_β + Fmoc H-*9* + Fmoc CH_2, 5H), 7.29–7.40 (Fmoc H-*2* and H-*7*, 2H), 7.42–7.47 (Fmoc H-*3* and H-*6*, 2H), 7.55–7.70 (Fmoc H-*1* and H-*8*, 2H), 7.73–7.85 (Fmoc H-*4* and H-*5*, 2H), 6.30–8.30 (b, COOH); ^{13}C NMR (100 MHz, $CDCl_3$ at 298 K): δ 28.29 (C(C$_3$)$_3$), 31.47/32.29 (NCH$_2$$CH_2$), 44.13/44.38 (N$CH_2CH_2$), 47.51/47.60 (Fmoc C-*9*), 62.73/62.95 (C_α), 67.96/68.13 (Fmoc CH_2), 71.77/72.67 (C_β), 75.34 (C (CH$_3$)$_3$), 120.33 (Fmoc C-*4* and C-*5*), 125.39/125.50/ 125.55/125.61 (Fmoc C-*1* and C-*8*), 127.46 (Fmoc C-*2* and C-*7*), 128.01/128.07 (Fmoc C-*3* and C-*6*), 141.58/ 141.66 (Fmoc C-*4′* and C-*5′*), 144.04/144.23/144.46 (Fmoc C-*1′* and C-*8′*), 154.95/155.32 (OCON), 175.19/ 175.65 (COOH).

5.8. (2*S*,3*R*)-3-*tert*-Butoxy-2-(2-diazoacetyl)pyrrolidine-1-carboxylic acid 9*H*-fluoren-9-ylmethyl ester (21)

Acid **20** (840 mg, 2.05 mmol) was dissolved with stirring in anhydrous dichloromethane (15 mL). The reaction was flushed with nitrogen and cooled to −15 °C. Isobutyl chloroformate (304 mg, 2.24 mmol) in anhydrous dichloromethane (2.5 mL) and *N*-methylmorpholine (420 mg, 4.10 mmol) in anhydrous dichloromethane (2.5 mL) were added simultaneously in 0.5 mL aliquots over 15 min. Etheral diazomethane (generated from the addition of diazald (4.7 g, ∼15 mmol in diethyl ether (75 mL)) onto sodium hydroxide (5.25 g) in water (7.5 mL)/ethanol (15 mL) at 60 °C) was added to the activated aminoacid solution and stirred at ambient temperature for 72 h. Acetic acid (∼2 mL) was added to quench the reaction, then *tert*-butylmethylether (150 mL) was added, the organics washed with water (3 × 200 mL),

then dried (Na_2SO_4). The solvents were removed in vacuo to give a thick yellow oil (1240 mg). The crude oil was purified over silica gel (75 g) eluting with a gradient of heptane–ethyl acetate $3:1 \rightarrow 2:1$. Desired fractions were combined and reduced in vacuo to give a pale yellow solid (210 mg, 24%). TLC (single UV spot, $R_f = 0.50$, heptane–ethyl acetate 1:1), analytical HPLC $t_R = 20.1$ min, HPLC–MS (two main UV peaks with $t_R = 7.5$ min, 350.1 $[M + H]^+$, 372.1 $[M + Na]^+$, 721.0 $[2M + Na]^+$ and $t_R = 9.9$ min, 406.2 $[M + H - N_2]^+$, 456.2 $[M + Na]^+$, 889.3 $[2M + Na]^+$). Note that upon HPLC–MS analysis, m/z 350.1 corresponds to the desired bicycle product (3aS,6aR)-3-oxo-hexahydro-furo[3,2-b]pyrrole-4-carboxylic acid 9H-fluoren-9-yl-methyl ester (**12**).

Also isolated were mixed anhydride of acid **20**, compound **37** (210 mg), TLC (single UV spot, $R_f = 0.70$, heptane–ethyl acetate 1:1), HPLC–MS (single main UV peak with $t_R = 12.1$ min, 532.2 $[M + Na]^+$); methyl ester of acid **20**, compound **38** (140 mg), TLC (single UV spot, $R_f = 0.65$, heptane–ethyl acetate 1:1), analytical HPLC $t_R = 21.2$ min, HPLC–MS (single main UV peak with $t_R = 10.5$ min, 424.2 $[M + H]^+$, 446.2 $[M + Na]^+$).

5.9. (–)-(3aS,6aR)-3-Oxo-hexahydrofuro[3,2-b]pyrrole-4-carboxylic acid 9H-fluoren-9-ylmethyl ester (12)

Diazomethylketone **21** (209 mg, 0.483 mmol) was treated with a solution of lithium chloride (205 mg, 4.8 mmol) in water (1.25 mL) and acetic acid (5.0 mL). Gas was evolved and the yellow oily solid dissolved over 1 h to give a virtually colourless solution. After 90 min, chloroform (150 mL) was added and the organics washed with $NaHCO_3$ (2×150 mL), brine (150 mL) and dried (Na_2SO_4). The solvents were removed in vacuo to give a thick yellow gum (200 mg). The crude gum was purified over silica gel (40 g) eluting with a gradient of heptane–ethyl acetate $3:2 \rightarrow 1:1$. Desired fractions were combined and reduced in vacuo to a white crystalline solid (133 mg, 19% from starting acid). TLC (single UV spot, $R_f = 0.25$, heptane–ethyl acetate 1:1), analytical HPLC broad peak $t_R = 15.2$–17.6 min, HPLC–MS (single broad UV peak with $t_R = 7.5$–8.6 min, 350.1 $[M + H]^+$, 372.1 $[M + Na]^+$, 721.2 $[2M + Na]^+$). Microanalysis indicated the presence of residual solvent following drying in vacuo and re-drying at elevated temperature lead to partial thermal decomposition. Exact mass calcd for $C_{21}H_{19}NO_4$ (MH$^+$): 350.1387, found 350.1401 (δ +4.02 ppm); $[\alpha]_D^{22}$ − 137.2 (c 0.349, CHCl$_3$). Analysis by ^{1}H and ^{13}C NMR showed the presence of rotamers around the 3° amide bond. ^{1}H NMR (400 MHz, CDCl$_3$ at 298 K): δ 1.61–1.97/2.10–2.15 (m, NCH$_2$CH_2, 2H), 3.32–3.45 (m, NCH_2CH$_2$, 1H), 3.66–3.75/3.85–3.95 (m, NCH_2CH$_2$, $2 \times 1/2$H), 3.95/4.10 (m, COCH_{2A} + COCH_{2B}, 2H), 4.15–4.30 (m, Fmoc H-9 + Fmoc CH_2, 3H), 4.40–4.60/4.80–4.92 (complex, CH_α + CH_β, 2H), 7.20–7.30 (Fmoc H-2 and H-7, 2H), 7.31–7.42 (Fmoc H-3 and H-6, 2H), 7.50–7.57/7.60–7.66 (Fmoc H-1 and H-8, 2H), 7.68–7.76 (Fmoc H-4 and H-5, 2H); ^{13}C NMR (100 MHz, CDCl$_3$ at 298 K): δ 31.76/32.28 (NCH$_2$CH_2), 45.59/45.95 (NCH_2CH$_2$),

47.64 (Fmoc C-9), 62.26/62.77 (C_α), 68.03/68.65 (Fmoc CH_2), 71.28 (COCH_2), 82.17/83.11 (C_β), 120.38 (Fmoc C-4 and C-5), 125.41/125.59/125.88 (Fmoc C-1 and C-8), 127.45/127.49 (Fmoc C-2 and C-7), 128.13 (Fmoc C-3 and C-6), 141.73 (Fmoc C-4′ and C-5′), 144.16/144/37/144.88 (Fmoc C-1′ and C-8′), 155.33 (OCON), 209.32 (COCH$_2$).

5.10. (2S,3S)-3-*tert*-Butoxy-pyrrolidine-1,2-dicarboxylic acid 2-allyl ester 1-(9H-fluoren-9-ylmethyl) ester (22)

Compound **16** (1.45 g, 3.7 mmol) was dissolved in anhydrous dichloromethane (20 mL) in a 50 mL glass pressure tube and cooled to −78 °C. Isobutylene (∼10 mL) was condensed into the solution and concd H_2SO_4 (100 μL) added. The tube was sealed and stirred at ambient temperature for 72 h. The sealed tube was cooled to −78 °C, N-methylmorpholine (200 μL, 1 equiv w.r.t. concd H_2SO_4) added and allowed to warm to ambient temperature, unsealed, with stirring over 2 h. Dichloromethane (75 mL) was added and the organics washed with $NaHCO_3$ (75 mL), then brine (75 mL) and dried (Na_2SO_4). The solvents were removed in vacuo to give a mobile pale tan oil (1.98 g). The crude oil was purified over silica gel (150 g) eluting with a gradient of heptane–ethyl acetate $4:1 \rightarrow 3:1$. Desired fractions were combined and reduced in vacuo to a thick clear oil (1.43 g, 86%). TLC (single UV spot, $R_f = 0.50$, heptane–ethyl acetate 2:1), analytical HPLC $t_R = 22.9$ min, HPLC–MS (single main UV peak with $t_R = 11.3$ min, 450.2 $[M + H]^+$, 472.2 $[M + Na]^+$, 921.4 $[2M + Na]^+$). Anal. Calcd for $C_{27}H_{31}NO_5$: C, 72.14; H, 6.95; N, 3.12. Found: C, 72.18; H, 7.06; N, 3.11. Exact mass calcd for $C_{27}H_{31}NO_5$ (MNa$^+$): 472.2094, found 472.2088 (δ −1.36 ppm).

5.11. (–)-(2S,3S)-3-*tert*-Butoxy-pyrrolidine-1,2-dicarb-oxylic acid 1-(9H-fluoren-9-ylmethyl) ester (23)

Compound **22** (1.37 g, 3.05 mmol) was dissolved in anhydrous dichloromethane (20 mL) with stirring. Tetrakis-triphenylphosphine palladium(0) (71 mg, 0.061 mmol, 0.02 equiv) was added, followed by phenyltrihydrosilane (0.66 g, 0.577 mL, 6.1 mmol, 2 equiv). After 2 h, dichloromethane (150 mL) was added and the organics washed with 0.01 N HCl (150 mL), brine (150 mL) and dried (Na_2SO_4). The solvents were removed in vacuo to give a dark grey solid (2.08 g). The crude solid was purified over silica gel (75 g) eluting with a gradient of heptane–ethyl acetate $2:1 \rightarrow 1:6$. Desired fractions were combined and reduced in vacuo to a white crystalline solid (500 mg, 40%). TLC (single UV spot, $R_f = 0.10$, heptane–ethyl acetate 1:2), analytical HPLC $t_R = 19.6$ min, HPLC–MS (single main UV peak with $t_R = 9.6$ min, 354.1 $[M + H - Bu^t]^+$, 410.2 $[M + H]^+$, 432.1 $[M + Na]^+$, 841.1 $[2M + Na]^+$). Microanalysis indicated the presence of residual solvent following drying in vacuo and re-drying at elevated temperature lead to partial thermal decomposition. Exact mass calcd for $C_{24}H_{27}NO_5$ (MNa$^+$): 432.1781, found 432.1786 (δ +0.99 ppm); $[\alpha]_D^{22}$ − 24.2 (c 0.409, CHCl$_3$). Analysis by ^{1}H and ^{13}C NMR showed the presence of rotamers around the 3° amide bond. ^{1}H NMR (400 MHz, CDCl$_3$

at 298 K): δ 1.14 (s, C(C*H₃*)₃, 9H), 1.72–1.84/1.90–2.08 (m, NCH₂C*H₂*, 2 × 1H), 3.57–3.64 (m, NC*H₂*CH₂, 2H), 4.01–4.42 (m, C*H*α + C*H*β + Fmoc H-*9* + Fmoc C*H₂*, 5H), 7.20–7.30 (Fmoc H-*2* and H-*7*, 2H), 7.31–7.38 (Fmoc H-*3* and H-*6*, 2H), 7.45–7.59 (Fmoc H-*1* and H-*8*, 2H), 7.60–7.73 (Fmoc H-*4* and H-*5*, 2H), 6.60–8.30 (b, COO*H*); ¹³C NMR (100 MHz, CDCl₃ at 298 K): δ 27.75 (C(*C*H₃)₃), 31.89/32.76 (NCH₂*C*H₂), 45.02/45.14 (N*C*H₂CH₂), 46.76 (Fmoc C-*9*), 67.01/67.69 (*C*α), 67.24/67.64 (Fmoc *C*H₂), 73.24/74.09 (*C*β), 74.91 (*C* (CH₃)₃), 119.55/119.65 (Fmoc C-*4* and C-*5*), 124.69/124.85 (Fmoc C-*1* and C-*8*), 126.64/126.73 (Fmoc C-*2* and C-*7*), 127.25/127.40 (Fmoc C-*3* and C-*6*), 140.93 (Fmoc C-*4′* and C-*5′*), 143.38/143.49/143.65 (Fmoc C-*1′* and C-*8′*), 154.22/155.67 (O*C*ON), 174.10/175.73 (*C*OOH).

5.12. (2*S*,3*S*)-3-*tert*-Butoxy-2-(2-diazoacetyl)pyrrolidine-1-carboxylic acid 9*H*-fluoren-9-ylmethyl ester (24)

Acid **23** (450 mg, 1.1 mmol) was dissolved with stirring in anhydrous dichloromethane (15 mL). The reaction was flushed with nitrogen and cooled to −15 °C. Isobutyl chloroformate (163 mg, 1.1 mmol) in anhydrous dichloromethane (2.5 mL) and *N*-methylmorpholine (225 mg, 2.2 mmol) in anhydrous dichloromethane (2.5 mL) were added simultaneously in 0.5 mL aliquots over 15 min. Etheral diazomethane (generated from the addition of diazald (4.7 g, ~15 mmol in diethyl ether (75 mL)) onto sodium hydroxide (5.25 g) in water (7.5 mL)/ethanol (15 mL) at 60 °C) was added to the activated aminoacid solution and stirred at ambient temperature for 1 h. Acetic acid (~2 mL) was added to quench the reaction, then *tert*-butylmethylether (150 mL) was added, the organics washed with water (3 × 200 mL), then dried (Na₂SO₄). The solvents were removed in vacuo to give a thick yellow gum (450 mg). TLC (single UV spot, R_f = 0.60, heptane–ethyl acetate 1:1), analytical HPLC t_R = 20.6 min (>85%), HPLC–MS (single main UV peak with t_R = 10.2 min, 406.2 [M + H − N₂]⁺, 456.2 [M + Na]⁺). Crude diazomethylketone **24** was used directly in the following reaction.

5.13. (2*S*,3*S*)-3-*tert*-Butoxy-2-(2-chloroacetyl)pyrrolidine-1-carboxylic acid 9*H*-fluoren-9-ylmethyl ester (25)

Crude diazomethylketone **24** (450 mg, ~1.05 mmol) was treated with a solution of lithium chloride (422 mg, 10 mmol) in water (2.5 mL) and acetic acid (10.0 mL) with stirring. After 90 min, chloroform (150 mL) was added and the organics washed with NaHCO₃ (2 × 150 mL), brine (150 mL) and dried (Na₂SO₄). The solvents were removed in vacuo to give a thick yellow oil (460 mg). The crude oil was purified over silica gel (75 g) eluting with a gradient of heptane–ethyl acetate 3:1 → 2:1. Desired fractions were combined and reduced in vacuo to a colourless oil (220 mg, 45% from starting acid). TLC (single UV spot, R_f = 0.45, heptane–ethyl acetate 2:1), analytical HPLC broad peak t_R = 22.1 min, HPLC–MS (single UV peak with t_R = 10.9 min, 442.1/444.1 [M + H]⁺). Analysis by ¹H and ¹³C NMR showed the presence of rotamers around the 3° amide bond. ¹³C NMR (100 MHz, CDCl₃ at 298 K): δ 28.75 (C(*C₃*)₃),

32.26/33.40 (NCH₂*C*H₂), 45.18/45.38 (N*C*H₂CH₂), 46.91/48.07 (CO*C*H₂Cl), 47.58/47.68 (Fmoc C-*9*), 66.65/68.12 (Fmoc *C*H₂), 71.35/72.02 (*C*α), 73.72/74.50 (*C*β), 75.92 (*C* (CH₃)₃), 120.40/120.48 (Fmoc C-*4* and C-*5*), 124.27/124.34 (Fmoc C-*1* and C-*8*), 127.49/127.52 (Fmoc C-*2* and C-*7*), 127.65/127.77 (Fmoc C-*3* and C-*6*), 141.67/141.71 (Fmoc C-*4′* and C-*5′*), 143.84/144.06 (Fmoc C-*1′* and C-*8′*), 154.59/155.70 (O*C*ON), 199.97/200.54 (*C*OCH₂Cl).

5.14. (±)-*cis*-3-Hydroxypiperidine-1,2-dicarboxylic acid 1-(9*H*-fluoren-9-ylmethyl) ester (28)

(±)-*cis*-3-Hydroxypiperidine-2-carboxylic acid **27** (obtained by hydrogenation of commercially available 3-hydroxypicolinic acid **26**[30]) (15.0 g, 103.4 mmol) was added to a vigorously stirred, ice-cooled solution of sodium carbonate (22.90 g, 217.1 mmol) in water (20 mL). 1,4-Dioxan (100 mL) was added providing a clear pale yellow solution. 9-Fluorenylmethyl chloroformate (27.52 g, 108.4 mmol) in 1,4-dioxan (100 mL) was added over 1 h, then the ice-cooling removed and the mixture stirred at ambient temperature for an additional 1 h. Additional water (150 mL) was added, the reaction mixture washed with chloroform (2 × 250 mL) and the combined organic layers discarded. The aqueous phase was acidified with 1 N HCl to ~pH 2, providing a thick opaque mixture. The acidified aqueous mixture was extracted with chloroform (2 × 500 mL) and the now clear aqueous phase discarded. The opaque combined chloroform layers were dried (Na₂SO₄), filtered and reduced in vacuo to provide a white foam (30.2 g, 79.5%). TLC (minor UV spot, R_f = 0.58, major UV spot R_f = 0.25, methanol–chloroform 1:4), analytical HPLC major peak t_R = 17.0 min, HPLC–MS (single major UV peak with t_R = 8.0 min), 368.0 [M + H]⁺, 390.0 [M + Na]⁺. Analysis by ¹H and ¹³C NMR showed the presence of rotamers around the 3° amide bond. ¹³C NMR (100 MHz, DMSO-*d₆* at 298 K): δ 23.29/23.57 (NCH₂*C*H₂CH₂), 28.89 (NCH₂CH₂*C*H₂), 40.19 (N*C*H₂CH₂CH₂), 47.59 (Fmoc C-*9*), 59.11/59.43 (*C*α), 67.34 (*C*β), 67.75/67.87 (Fmoc *C₂*), 121.13 (Fmoc C-*4* and C-*5*), 126.90/127.02 (Fmoc C-*1* and C-*8*), 128.11 (Fmoc C-*2* and C-*7*), 128.68 (Fmoc C-*3* and C-*6*), 141.73 (Fmoc C-*4′* and C-*5′*), 144.58/144.76 (Fmoc C-*1′* and C-*8′*), 155.71/156.23 (O*C*ON), 172.37/172.63 (*C*OOH).

5.15. (±)-*cis*-3-Hydroxypiperidine-1,2-dicarboxylic acid 2-allyl ester 1-(9*H*-fluoren-9-ylmethyl) ester (29)

Compound **28** (28.2 g, 76.7 mmol) was dissolved in (200 mL) in a Dean–Stark apparatus. Allyl alcohol (50 mL) was added followed by *p*-toluenesulfonic acid hydrate (15.1 g, 78.2 mmol). The mixture was refluxed for 1 h, cooled and CHCl₃ (500 mL) added. The organic layer was washed with NaHCO₃ (2 × 250 mL), 0.1 N HCl (250 mL) and brine (250 mL), then dried (Na₂SO₄). Filtration and reduction in vacuo gave a pale yellow mobile oil (35 g). The crude oil was purified over silica gel (240 g) eluting with a gradient of heptane–ethyl acetate 3:1 → 1:1. Desired fractions were combined and reduced in vacuo to a colourless gum (20.4 g, 65%). TLC (single

UV spot, R_f = 0.20, heptane–ethyl acetate 2:1), analytical HPLC t_R = 20.0 min, HPLC–MS (single main UV peak with t_R = 9.5 min), 408.1 $[M + H]^+$, 430.1 $[M + Na]^+$. Anal. Calcd for $C_{24}H_{25}NO_5$: C, 70.74; H, 6.18; N, 3.44. Found: C, 70.65; H, 6.18; N, 3.40. Analysis by ^1H and ^{13}C NMR showed the presence of rotamers around the 3° amide bond. ^{13}C NMR (100 MHz, CDCl$_3$ at 298 K): δ 23.87/24.11 (NCH$_2$CH$_2$CH$_2$), 30.59 (NCH$_2$CH$_2$CH$_2$), 41.26/41.56 (NCH$_2$CH$_2$CH$_2$), 47.62 (Fmoc C-9), 58.29/59.54 ($C_α$), 66.44/66.54 (OCH$_2$CH=CH$_2$), 68.28 (Fmoc C_2), 69.14/69.42 ($C_β$), 119.67/119.90 (OCH$_2$CH=CH$_2$), 120.43 (Fmoc C-4 and C-5), 125.22/125.35 (Fmoc C-1 and C-8), 127.48 (Fmoc C-2 and C-7), 128.15 (Fmoc C-3 and C-6), 131.43/131.57 (OCH$_2$CH=CH$_2$), 141.73 (Fmoc C-4′ and C-5′), 144.19/144.38 (Fmoc C-1′ and C-8′), 155.67/156.27 (OCON), 171.56 (COOCH$_2$CH=CH$_2$).

5.16. Enzymic resolution of (±)-*cis*-3-hydroxypiperidine-1,2-dicarboxylic acid 2-allyl ester 1-(9*H*-fluoren-9-yl-methyl) ester (29) to (+)-(2*R*,3*S*)-3-hydroxypiperidine-1,2-dicarboxylic acid 2-allyl ester 1-(9*H*-fluoren-9-ylmethyl) ester (30) and (+)-(2*S*,3*R*)-3-acetoxypiperidine-1,2-dicarboxylic acid 2-allyl ester 1-(9*H*-fluoren-9-ylmethyl) ester (31)

Racemate **29** (19.6 g, 48.1 mmol), Lipase PS (25 g, ex Amano Enzyme Inc.), vinyl acetate (300 mL) and diisopropyl ether (200 mL) were stirred at 30 °C. After five days HPLC indicated no further change, giving two peaks (52.5:47.5%, indicating 95% conversion) and the reaction mixture was filtered through Celite (3 cm × 10 cm bed). The Celite bed was washed with chloroform (3 × 250 mL) and the combined organic filtrate reduced in vacuo to a viscous tan oil (23.0 g). The crude oil was purified over silica gel (300 g) eluting with a gradient of heptane–ethyl acetate 3:1 → 1:2 giving two major fractions. Fraction 1 was combined and reduced in vacuo to give compound (+)-(**31**) as a viscous very pale yellow oil (9.5 g, 44%). TLC (single UV spot, R_f = 0.40, heptane–ethyl acetate 2:1), analytical HPLC t_R = 22.6 min, HPLC–MS (single main UV peak with t_R = 10.7 min, 450.1 $[M + H]^+$, 472.1 $[M + Na]^+$). Anal. Calcd for $C_{26}H_{27}NO_6$: C, 69.47; H, 6.05; N, 3.12. Found: C, 69.40; H, 6.32; N, 3.01. Exact mass calcd for $C_{26}H_{27}NO_6$ (MH$^+$): 450.1911, found 450.1929 (δ +3.99 ppm); $[α]_D^{22}$ + 14.6 (*c* 0.52, CHCl$_3$) (lit.[31] $[α]_D^{20}$ + 12.8 (*c* 1.1, CH$_2$Cl$_2$)). Analysis by ^1H and ^{13}C NMR showed the presence of rotamers around the 3° amide bond. ^1H NMR (400 MHz, CDCl$_3$ at 298 K): δ 1.25–1.32/1.52–1.70/1.72–2.00 (m, NCH$_2$CH$_2$CH$_2$ + NCH$_2$CH$_2$CH$_2$, 4H), 2.05–2.15 (br s, OCOCH$_3$, 3H), 3.35–3.58 (m, NCH$_2$CH$_2$CH$_2$, 1H), 3.98–4.10/4.18–4.22 (m, NCH$_2$CH$_2$CH$_2$, 1H), 4.24–4.31 (m, Fmoc H-9), 4.32–4.52 (m, Fmoc CH$_2$, 2H), 4.60–4.82 (m, OCH$_2$CH=CH$_2$, 2H), 4.92–4.99 (m, CH$_β$, 1H), 5.22–5.32 (m, CH$_α$, 1H), 5.28–5.32/5.34–5.41 (d, J = 17.20 Hz, COOCH$_2$CH=CH$_2$, 2H), 5.89–6.00 (m, OCH$_2$CH=CH$_2$, 1H), 7.30–7.37 (Fmoc H-2 and H-7, 2H), 7.38–7.46 (Fmoc H-3 and H-6, 2H), 7.59–7.76 (Fmoc H-1 and H-8, 2H), 7.78–7.80 (Fmoc H-4 and H-5, 2H); ^{13}C NMR (100 MHz, CDCl$_3$ at 298 K): δ 21.22 (OCOCH$_3$), 23.01 (NCH$_2$C$_2$CH$_2$), 25.54

(NCH$_2$CH$_2$CH$_2$), 40.51/40.88 (NCH$_2$CH$_2$CH$_2$), 47.44 (Fmoc C-9), 55.55 ($C_α$), 66.08 (OCH$_2$CH=CH$_2$), 68.30/68.65 (Fmoc CH$_2$), 69.21/69.59 ($C_β$), 118.94/119.22 (OCH$_2$CH=CH$_2$), 120.31 (Fmoc C-4 and C-5), 125.34/125.49 (Fmoc C-1 and C-8), 127.43 (Fmoc C-2 and C-7), 128.04 (Fmoc C-3 and C-6), 131.93 (OCH$_2$CH=CH$_2$), 141.61 (Fmoc C-4′ and C-5′), 144.15 (Fmoc C-1′ and C-8′), 155.50/156.36 (OCON), 169.42/169.91/170.37 (OCOCH$_3$ + COOCH$_2$-CH=CH$_2$).

Fraction 1 was combined and reduced in vacuo to give compound (+)-(**30**), which was isolated as a white crystalline solid (9.05 g, 46%). TLC (single UV spot, R_f = 0.20, heptane–ethyl acetate 2:1), analytical HPLC t_R = 20.0 min, HPLC–MS (single main UV peak with t_R = 9.5 min, 408.1 $[M + H]^+$, 430.1 $[M + Na]^+$). Anal. Calcd for $C_{24}H_{25}NO_5$: C, 70.74; H, 6.18; N, 3.44. Found: C, 70.84; H, 6.20; N, 3.44. Exact mass calcd for $C_{24}H_{25}NO_5$ (MH$^+$): 408.1805, found 408.1825 (δ +4.70 ppm); $[α]_D^{22}$ + 38.8 (*c* 0.407, CHCl$_3$) (lit.[31] $[α]_D^{20}$ + 36.8 (*c* 1.2, CH$_2$Cl$_2$)). Analysis by ^1H and ^{13}C NMR showed the presence of rotamers around the 3° amide bond. ^1H NMR (400 MHz, CDCl$_3$ at 298 K): δ 1.47–1.61 (m, NCH$_2$CH$_2$CH$_2$ + NCH$_2$CH$_2$CH$_2$2H), 1.71–1.81 (m, NCH$_2$CH$_2$CH$_2$, 1H), 2.02–2.11 (m, NCH$_2$CH$_2$CH$_2$, 1H), 2.71–2.81/2.84–2.94 (m, NCH$_2$CH$_2$CH$_2$, 1H), 3.54–3.59 (m, CH$_β$, 1H), 3.70–3.82 (b, OH), 3.93–3.96/4.10–4.16/4.11 (m, NCH$_2$CH$_2$CH$_2$, 1H), 4.24–4.31 (m, Fmoc H-9), 4.40–4.56 (m, Fmoc CH$_2$, 2H), 4.61–4.78 (m, OCH$_2$CH=CH$_2$, 2H), 4.98/5.18 (d, J = 5.00, 4.85 Hz, CH$_α$, 1H), 5.25–5.37 (m, COOCH$_2$CH=CH$_2$, 2H), 5.86–5.96 (m, OCH$_2$ CH=CH$_2$, 1H), 7.30–7.34 (Fmoc H-2 and H-7, 2H), 7.41–7.48 (Fmoc H-3 and H-6, 2H), 7.53–7.62 (Fmoc H-1 and H-8, 2H), 7.79–7.81 (Fmoc H-4 and H-5, 2H); ^{13}C NMR (100 MHz, CDCl$_3$ at 298 K): δ 23.87/24.12 (NCH$_2$CH$_2$CH$_2$), 30.60 (NCH$_2$-CH$_2$CH$_2$), 41.27/41.57 (NCH$_2$CH$_2$CH$_2$), 47.62 (Fmoc C-9), 58.29/59.54 ($C_α$), 66.44/66.54 (OCH$_2$CH=CH$_2$), 68.28 (Fmoc CH$_2$), 69.15/69.42 ($C_β$), 119.67/119.91 (OCH$_2$CH=CH$_2$), 120.42 (Fmoc C-4 and C-5), 125.22/125.35 (Fmoc C-1 and C-8), 127.48 (Fmoc C-2 and C-7), 128.15 (Fmoc C-3 and C-6), 131.42/131.57 (OCH$_2$CH=CH$_2$), 141.73 (Fmoc C-4′ and C-5′), 144.12/144.37 (Fmoc C-1′ and C-8′), 155.67/156.26 (OCON), 171.57 (COOCH$_2$CH=CH$_2$).

5.17. (–)-(2*S*,3*R*)-3-Hydroxypiperidine-1,2-dicarboxylic acid 2-allyl ester 1-(9*H*-fluoren-9-ylmethyl) ester (32)

Compound **31** (4.5 g, 10 mmol) was dissolved in allyl alcohol (50 mL), concd H$_2$SO$_4$ (200 μL) added and heated to reflux for 24 h. The mixture was cooled, EtOAc (250 mL) added and washed with NaHCO$_3$ (250 mL), brine (250 mL) and dried (Na$_2$SO$_4$). The solvents were removed in vacuo to give a tan oil (4.2 g). The crude oil was purified over silica gel (170 g) eluting with a gradient of heptane–ethyl acetate 3:1 → 1:1. Desired fractions were combined and reduced in vacuo to a white crystalline solid (3.0 g, 74%). TLC (single UV spot, R_f = 0.20, heptane–ethyl acetate 2:1), analytical HPLC t_R = 19.5 min, HPLC–MS (single main UV

peak with $t_R = 9.5$ min, 408.2 [M + H]$^+$, 430.2 [M + Na]$^+$). Anal. Calcd for $C_{24}H_{25}NO_5$: C, 70.74; H, 6.18; N, 3.44. Found: C, 70.75; H, 6.18; N, 3.37. Exact mass calcd for $C_{24}H_{25}NO_5$ (MH$^+$): 408.1805, found 408.1823 (δ +4.36 ppm); $[\alpha]_D^{22}$ − 42.8 (*c* 0.407, CHCl$_3$) (lit.[31] $[\alpha]_D^{20}$ − 33.6 (*c* 1.5, CH$_2$Cl$_2$)). Analysis by ^{1}H and ^{13}C NMR showed the presence of rotamers around the 3° amide bond. ^{1}H NMR (400 MHz, CDCl$_3$ at 298 K): δ 1.46–1.59 (m, NCH$_2$ C*H*$_2$CH$_2$ + NCH$_2$CH$_2$-C*H*$_2$, 2H), 1.74–1.81 (m, NCH$_2$C*H*$_2$CH$_2$, 1H), 2.01–2.10 (m, NCH$_2$CH$_2$C*H*$_2$, 1H), 2.70–2.82/2.88–2.99 (m, NC*H*$_2$CH$_2$CH$_2$, 1H), 3.49–3.62 (m, C*H*$_\beta$, 1H), 3.70–3.80 (b, O*H*), 3.90–3.94/4.09–4.14 (m, NC*H*$_2$CH$_2$CH$_2$, 1H), 4.26–4.32 (m, Fmoc H-*9*), 4.41–4.58 (m, Fmoc C*H*$_2$, 2H), 4.60–4.80 (m, OC*H*$_2$CH=CH$_2$, 2H), 4.96–4.98/5.17–5.18 (dd, *J* = 4.95, 4.85 Hz, C*H*$_\alpha$, 1H), 5.25–5.42 (m, COOCH$_2$CH=C*H*$_2$, 2H), 5.82–5.97 (m, OCH$_2$C*H*=CH$_2$, 1H), 7.30–7.38 (Fmoc H-*2* and H-*7*, 2H), 7.42–7.48 (Fmoc H-*3* and H-*6*, 2H), 7.55–7.63 (Fmoc H-*1* and H-*8*, 2H), 7.79–7.84 (Fmoc H-*4* and H-*5*, 2H); ^{13}C NMR (100 MHz, CDCl$_3$ at 298 K): δ 23.86/24.12 (NCH$_2$*C*H$_2$CH$_2$), 30.62 (NCH$_2$CH$_2$*C*H$_2$), 41.28/41.57 (N*C*H$_2$CH$_2$CH$_2$), 47.62 (Fmoc C-*9*), 58.29/59.54 (*C*$_\alpha$), 66.43/66.54 (O*C*H$_2$CH=CH$_2$), 68.27 (Fmoc *C*$_2$), 69.15/69.43 (*C*$_\beta$), 119.69/119.91 (OCH$_2$CH=*C*H$_2$), 120.42 (Fmoc C-*4* and C-*5*), 125.22/125.35 (Fmoc C-*1* and C-*8*), 127.47 (Fmoc C-*2* and C-*7*), 128.14 (Fmoc C-*3* and C-*6*), 131.43/131.57 (OCH$_2$*C*H=CH$_2$), 141.73 (Fmoc C-*4'* and C-*5'*), 144.12/144.37 (Fmoc C-*1'* and C-*8'*), 155.67/156.26 (O*C*ON), 171.57 (*C*OOCH$_2$-CH=CH$_2$).

5.18. (+)-(2*S*,3*R*)-3-*tert*-Butoxypiperidine-1,2-dicarboxylic acid 2-allyl ester 1-(9*H*-fluoren-9-ylmethyl) ester (33)

Compound **32** (1.75 g, 4.30 mmol) was dissolved in anhydrous dichloromethane (20 mL) in a 50 mL glass pressure tube and cooled to −78 °C. Isobutylene (∼10 mL) was condensed into the solution and concd H$_2$SO$_4$ (100 µL) added. The tube was sealed, the cooling removed and stirred at ambient temperature for 72 h. The sealed tube was cooled to −78 °C, *N*-methylmorpholine (200 µL, 1 equiv w.r.t. concd H$_2$SO$_4$) and allowed to warm to ambient temperature, unsealed, with stirring over 2 h. Dichloromethane (75 mL) was added and the organics washed with NaHCO$_3$ (75 mL), then brine (75 mL) and dried (Na$_2$SO$_4$). The solvents were removed in vacuo to give a pale tan oil (1.91 g). The crude oil was purified over silica gel (100 g) eluting with a gradient of heptane–ethyl acetate 5:1 → 3:1. Desired fractions were combined and reduced in vacuo to a viscous clear oil (1.59 g, 80%). TLC (single UV spot, $R_f = 0.50$, heptane–ethyl acetate 2:1), analytical HPLC $t_R = 24.1$ min, HPLC–MS (single main UV peak with $t_R = 11.9$ min, 408.2 [M + H − Bu^t]$^+$, 486.3 [M + Na]$^+$, 949.5 [2M + Na]$^+$); $[\alpha]_D^{22}$ + 24.4 (*c* 0.492, CHCl$_3$). Analysis by ^{1}H and ^{13}C NMR showed the presence of rotamers around the 3° amide bond. ^{1}H NMR (400 MHz, CDCl$_3$ at 298 K): δ 1.23 (s, C(C*H*$_3$)$_3$, 9H), 1.46–1.98 (m, NCH$_2$C*H*$_2$CH$_2$ + NCH$_2$CH$_2$C*H*$_2$, 4H), 3.37–3.45/3.46–3.57 (m, NC*H*$_2$CH$_2$CH$_2$, 1H), 3.61–3.72 (m, C*H*$_\beta$, 1H), 3.90–3.99/4.02–4.10 (dt, NC*H*$_2$CH$_2$CH$_2$,

1H), 4.20–4.72 (m, Fmoc H-*9* + Fmoc C*H*$_2$+ OC*H*$_2$CH=CH$_2$, 5H), 4.89/5.01 (dd, *J* = 6.35 Hz, C*H*$_\alpha$, 1H), 5.24 (d, *J* = 10.45 Hz, COOCH$_2$CH=C*H*$_2$, 1H), 5.38 (d, *J* = 17.35 Hz, OCH$_2$CH=C*H*$_2$, 1H), 5.88–5.99 (m, OCH$_2$C*H*=CH$_2$, 1H), 7.29–7.36 (Fmoc H-*2* and H-*7*, 2H), 7.38–7.47 (Fmoc H-*3* and H-*6*, 2H), 7.56–7.69 (Fmoc H-*1* and H-*8*, 2H), 7.76–7.81 (Fmoc H-*4* and H-*5*, 2H); ^{13}C NMR (100 MHz, CDCl$_3$ at 298 K): δ 23.69/23.99 (NCH$_2$*C*$_2$CH$_2$), 28.38/28.65 (*C*(CH$_3$)$_3$), 28.75 (NCH$_2$CH$_2$*C*H$_2$), 40.40/40.72 (N*C*H$_2$CH$_2$CH$_2$), 47.61 (Fmoc C-*9*), 58.36/58.47 (*C*$_\alpha$), 65.67 (O*C*H$_2$CH=CH$_2$), 67.82 (*C*$_\beta$), 67.99/68.13 (Fmoc *C*$_2$), 74.97 (*C* (CH$_3$)$_3$), 118.44/118.57 (OCH$_2$CH=*C*$_2$), 120.40 (Fmoc C-*4* and C-*5*), 125.39/125.48 (Fmoc C-*1* and C-*8*), 127.46 (Fmoc C-*2* and C-*7*), 128.10 (Fmoc C-*3* and C-*6*), 132.49 (OCH$_2$ *C*H=CH$_2$), 141.71 (Fmoc C-*4'* and C-*5'*), 144.14/144.30 (Fmoc C-*1'* and C-*8'*), 155.44/157.00 (O*C*ON), 170.43/171.05 (*C*OOCH$_2$-CH=CH$_2$).

5.19. (+)(2*S*,3*R*)-3-*tert*-Butoxypiperidine-1,2-dicarboxylic acid 1-(9*H*-fluoren-9-ylmethyl) ester (34)

Compound **33** (1.52 g, 3.29 mmol) was dissolved in anhydrous dichloromethane (25 mL) with stirring. Tetrakistriphenylphosphine palladium(0) (76 mg, 0.066 mmol, 0.02 equiv) was added, followed by phenyltrihydrosilane (0.71 g, 0.622 mL, 6.58 mmol, 2 equiv). After 1 h, dichloromethane (150 mL) was added and the organics washed with 0.01 N HCl (150 mL), brine (150 mL) and dried (Na$_2$SO$_4$). The solvents were removed in vacuo to give a dark grey solid (2.05 g). The crude solid was purified over silica gel (75 g) eluting with a gradient of heptane–ethyl acetate 2:1 → 1:2. Desired fractions were combined and reduced in vacuo to a white crystalline solid (0.97 g, 70%). TLC (single UV spot, $R_f = 0.25$, heptane–ethyl acetate 1:1), analytical HPLC $t_R = 21.3$ min, HPLC–MS (single main UV peak with $t_R = 10.3$ min, 368.2 [M + H − Bu^t]$^+$, 446.2 [M + Na]$^+$, 869.3 [2M + Na]$^+$). Microanalysis indicated the presence of residual solvent following drying in vacuo and re-drying at elevated temperature lead to partial thermal decomposition. Exact mass calcd for $C_{25}H_{29}NO_5$ (MNa$^+$): 446.1938, found 446.1953 (δ +3.36 ppm); $[\alpha]_D^{22}$ + 21.5 (*c* 0.423, CHCl$_3$).

5.20. (2*S*,3*R*)-3-*tert*-Butoxy-2-(2-diazoacetyl)piperidine-1-carboxylic acid 9*H*-fluoren-9-ylmethyl ester (35)

Acid **34** (830 mg, 1.96 mmol) was dissolved with stirring in anhydrous dichloromethane (20 mL). The reaction was flushed with nitrogen and cooled to −15 °C. Isobutyl chloroformate (296 mg, 2.16 mmol) in anhydrous dichloromethane (2.5 mL) and *N*-methylmorpholine (397 mg, 3.92 mmol) in anhydrous dichloromethane (2.5 mL) were added simultaneously in 0.5 mL aliquots over 15 min. Etheral diazomethane (generated from the addition of diazald (2.5 g, ∼8 mmol in diethyl ether (40 mL)) onto sodium hydroxide (2.75 g) in water (4.3 mL)/ethanol (8.6 mL) at 60 °C) was added to the activated aminoacid solution and stirred at ambient

temperature for 24 h. Acetic acid (∼2 mL) was added to quench the reaction, then *tert*-butylmethylether (100 mL) was added, the organics washed with water (3 × 150 mL), then dried (Na$_2$SO$_4$). The solvents were removed in vacuo to give a thick yellow oil (1.02 g). The crude oil was used for the next stage without purification. TLC (single main UV spot, R_f = 0.40, heptane–ethyl acetate 2:1), analytical HPLC t_R = 18.9 min (50.8%) plus numerous minor peaks, HPLC–MS (two main UV peaks with t_R = 9.1 min, 364.2 [M + H]$^+$, 749.2 [2M + Na]$^+$ and t_R = 10.9 min, 420.2 [M + H − N$_2$]$^+$, 470.2 [M + Na]$^+$, 917.3 [2M + Na]$^+$). Note that upon HPLC–MS analysis, *m/z* 364.2 corresponds to the desired bicycle product (3a*S*,7a*R*)-3-oxo-hexahydrofuro[3,2-*b*]pyridine-4-carboxylic acid 9*H*-fluoren-9-ylmethyl ester.

5.21. (–)-(3a*S*,7a*R*)-3-Oxo-hexahydrofuro[3,2-*b*]pyridine-4-carboxylic acid 9*H*-fluoren-9-ylmethyl ester (13)

A solution of lithium chloride (844 mg, 20 mmol) in water (5 mL) and acetic acid (20 mL) was added to compound **35** (1.0 g, ∼2 mmol). Gas was evolved and the yellow oily solid dissolved over 1 h to give a virtually colourless solution. After 90 min, chloroform (150 mL) was added and the organics washed with NaHCO$_3$ (2 × 150 mL), brine (150 mL) and dried (Na$_2$SO$_4$). The solvents were removed in vacuo to give a pale yellow gum (920 mg). The crude gum was purified over silica gel (135 g) eluting with a gradient of heptane–ethyl acetate 3:1 → 1:1. Desired fractions were combined and reduced in vacuo to a white crystalline solid (370 mg, 52% from starting acid). TLC (single UV spot, R_f = 0.25, heptane–ethyl acetate 2:1), analytical HPLC t_R = 18.7 min, HPLC–MS (single UV peak with t_R = 9.1 min, 364.2 [M + H]$^+$, 386.2 [M + Na]$^+$). Microanalysis indicated the presence of residual solvent following drying in vacuo and re-drying at elevated temperature lead to partial thermal decomposition. Exact mass calcd for C$_{22}$H$_{21}$NO$_4$ (MH$^+$): 364.1543, found 364.1554 (δ +3.03 ppm); [α]$_D^{22}$ − 13.5 (*c* 0.363, CHCl$_3$). Analysis by ^{1}H and ^{13}C NMR showed the presence of rotamers around the 3° amide bond. ^{1}H NMR (400 MHz, CDCl$_3$ at 298 K): δ 1.29–1.49 (m, NCH$_2$C*H*$_2$CH$_2$ + NCH$_2$CH$_2$C*H*$_2$, 2H), 1.61–1.80 (m, NCH$_2$C*H*$_2$CH$_2$, 1H), 2.06–2.19 (m, NCH$_2$CH$_2$C*H*$_2$, 1H), 2.50–2.62/2.63–2.80 (m, NCH$_2$CH$_2$CH$_2$, 1H), 3.96 (b, NC*H*$_2$CH$_2$CH$_2$, 1H), 3.97 (d, *J* = 16.25 Hz, COC*H*$_{2A}$, 1H), 4.15 (m, Fmoc H-*9*, CH$_β$, 1H), 4.25–4.34 (m, CH$_β$, 1H), 4.36–4.60 (br m, Fmoc C*H*$_2$ + COC*H*$_{2B}$, 3H), 4.75–4.82/5.11–5.19 (b, C*H*$_α$, 1H), 7.30–7.36 (Fmoc H-*2* and H-*7*, 2H), 7.41–7.49 (Fmoc H-*3* and H-*6*, 2H), 7.52–7.68 (Fmoc H-*1* and H-*8*, 2H), 7.75–7.85 (Fmoc H-*4* and H-*5*, 2H); ^{13}C NMR (100 MHz, CDCl$_3$ at 298 K): δ 21.75/22.04 (NCH$_2$CH$_2$CH$_2$), 26.60 (NCH$_2$CH$_2$CH$_2$), 41.40/41.66 (NCH$_2$CH$_2$CH$_2$), 47.59 (Fmoc C-*9*), 60.42 (C$_α$), 67.54 (Fmoc CH$_2$), 68.21/68.39 (COCH$_2$), 72.61 (C$_β$), 120.39, (Fmoc C-*4* and C-*5*), 125.43 (Fmoc C-*1* and C-*8*), 127.51 (Fmoc C-*2* and C-*7*), 128.14 (Fmoc C-*3* and C-*6*), 141.73 (Fmoc C-*4′* and C-*5′*), 144.30 (Fmoc C-*1′* and C-*8′*), 155.79/156.35 (OCON), 211.10/211.4 (COCH$_2$).

6. Solid phase chemistry

6.1. Preparation of (3a*S*,6a*R*)-3-oxo-hexahydrofuro[3,2-*b*]pyrrole-4-carboxylic acid 9*H*-fluoren-9-ylmethyl ester—linker construct (43a)

Building block **12** (100 mg, 0.286 mmol, 1 equiv) was dissolved in a mixture of ethanol (5.0 mL) and water (0.75 mL) containing sodium acetate·trihydrate (59 mg, 0.428 mmol, 1.5 equiv). 4-{[(Hydrazinocarbonyl)amino]methyl}cyclohexane carboxylic acid trifluoroacetate (95 mg, 0.286 mmol, 1.0 equiv)[33] was added and the mixture was heated for 90 min at 86 °C then allowed to cool to ambient temperature and diluted with chloroform (50 mL). The chloroform layer was washed with dilute aqueous hydrochloric acid (pH 3, 2 × 50 mL), brine (50 mL), dried (Na$_2$SO$_4$) and evaporated in vacuo to give (**43a**) as a colourless gum (172 mg). Analytical HPLC gave two main peaks at t_R = 16.5 min and 18.5 min (mixture of *E*- and *Z*-isomers), HPLC–MS (main UV peaks with t_R = 7.8 and 8.8 min, 547.3 [M + H]$^+$, 569.3 [M + Na]$^+$). Crude **43a** was used directly for construct loading.

6.2. Preparation of (3a*S*,7a*R*)-3-oxo-hexahydrofuro[3,2-*b*]pyridine-4-carboxylic acid 9*H*-fluoren-9-ylmethyl ester—linker construct (44a)

Building block **13** (250 mg, 0.689 mmol, 1 equiv) was dissolved in a mixture of ethanol (12.0 mL) and water (1.75 mL) containing sodium acetate·trihydrate (141 mg, 1.03 mmol, 1.5 equiv). 4-{[(Hydrazinocarbonyl)amino]methyl}cyclohexane carboxylic acid trifluoroacetate (227 mg, 0.689 mmol, 1.0 equiv)[33] was added and the mixture was heated for 4 h at 86 °C then allowed to cool to ambient temperature and diluted with chloroform (150 mL). The chloroform layer was washed with dilute aqueous hydrochloric acid (pH 3, 2 × 75 mL), brine (75 mL), dried (Na$_2$SO$_4$) and evaporated in vacuo to give (**44a**) as a clear syrup (450 mg). Analytical HPLC gave two main peaks at 17.10 and 18.6 min (mixture of *E*- and *Z*-isomers), HPLC–MS (main UV peaks with t_R = 8.0 and 9.0 min, 561.2 [M + H]$^+$). Crude **44a** was used directly for construct loading.

6.3. Solid phase protocols

Example inhibitors (**10**, **45a**–**e** and **11**, **46**) were prepared from constructs **43a** and **44a** by solid phase assembly techniques utilising multipins and standard Fmoc chemistry protocols.[34,43] Polyamide crowns with 10 μmol loading (SPMDINOF) were used for scale-up synthesis and purification of selected examples.[35] Constructs **43a** and **44a**, 3 equiv w.r.t. solid phase surface loading, were coupled overnight onto the 10 μmol crowns using standard 3 equiv HBTU, 3 equiv HOBt and 6 equiv NMM pre-activation (5 min) in a minimum volume of dimethylformamide to provide loaded constructs **43b** and **44b**. Constructs **43b** and **44b** were utilised in standard rounds of washing, Fmoc deprotection and coupling, followed by acidolytic cleavage to give crude inhibitors (**10**,

45a–**e** and **11**, **46**).[34] Examples were purified by semi-preparative HPLC (see general methods) and appropriate fractions combined and lyophilised into pre-tared glass vials. Purified analogues were then weighed and a volume of dimethylsulfoxide added as appropriate to give 10 mM stock solutions used for general storage and inhibition assays.

Each purified analogue was analysed giving the following characterisation data:

6.4. (3aS,6aR)-N-[3-Methyl-1S-(3-oxo-hexahydrofuro-[3,2-b]pyrrole-4-carbonyl)-butyl]-4-(4-methyl-piperazin-1-yl)benzamide (45a)

HPLC t_R = 10.0 min (main peak with 96% of total UV absorbance at 215 nm), HPLC–MS 443.3 [M + H]$^+$, 461.3 [M + H + 18]$^+$. Exact mass calcd for $C_{24}H_{34}N_4O_4$ (MH$^+$): 443.2653, found 443.2666 (δ + 3.07 ppm).

6.5. (3aS,6aR)-4-tert-Butyl-N-[3-methyl-1S-(3-oxo-hexahydrofuro[3,2-b]pyrrole-4-carbonyl)butyl]benzamide (10)

HPLC t_R = 17.4–18.8 min (95%), HPLC–MS 401.3 [M + H]$^+$. Exact mass calcd for $C_{23}H_{32}N_2O_4$ (MNa$^+$): 423.2254, found 423.2269 (δ + 3.41 ppm).

6.6. (3aS,6aR)-Furan-3-carboxylic acid [1S-cyclohexyl-methyl-2-oxo-2-(3-oxo-hexahydrofuro[3,2-b]pyrrol-4-yl)-ethyl]amide (45b)

HPLC t_R = 15.0–16.6 min (97%), HPLC–MS 391.2 [M + H]$^+$, 409.2 [M + H + 18]$^+$. Exact mass calcd for $C_{20}H_{26}N_2O_4S$ (MNa$^+$): 413.1505, found 413.1524 (δ + 4.37 ppm).

6.7. (3aS,6aR)-3-Bromo-N-[1S-(4-hydroxybenzyl)-2-oxo-2-(3-oxo-hexahydrofuro [3,2-b]pyrrol-4-yl)ethyl]benzamide (45c)

HPLC t_R = 12.5–14.0 min (96%), HPLC–MS 473.5/475.5 [M + H]$^+$. Exact mass calcd for $C_{22}H_{21}$-N_2O_5Br (MH$^+$): 473.0707, found 473.0725 (δ + 3.91 ppm).

6.8. (3aS,6aR)-3-Aminomethyl-N-[3-methyl-1S-(3-oxo-hexahydrofuro[3,2-b]pyrrole-4-carbonyl)butyl]benzamide (45d)

HPLC t_R = 9.2 min (97%), HPLC–MS 374.2 [M + H]$^+$, 392.2 [M + H + 18]$^+$. Exact mass calcd for $C_{20}H_{27}N_3O_4$ (MH$^+$): 374.2074, found 374.2090 (δ + 4.13 ppm).

6.9. (3aS,6aR)-4-tert-Butyl-N-[1S-(4-hydroxybenzyl)-2-oxo-2-(3-oxo-hexahydrofuro[3,2-b]pyrrol-4-yl)-ethyl]-benzamide (45e)

HPLC t_R = 15.0–17.0 min (96%), HPLC–MS 451.2 [M + H]$^+$, 469.2 [M + H + 18]$^+$. Exact mass calcd for $C_{26}H_{30}N_2O_5$ (MH$^+$): 451.2227, found 451.2248 (δ + 4.56 ppm).

6.10. (3aS,7aR)-4-tert-Butyl-N-[3-methyl-1S-(3-oxo-hexahydrofuro[3,2-b]pyridine-4-carbonyl)butyl]benzamide (11)

HPLC t_R = 19.0–20.0 min (94%), HPLC–MS 415.3 [M + H]$^+$, 851.5 [2M + Na]$^+$. Exact mass calcd for $C_{24}H_{34}N_2O_4$ (MH$^+$): 415.2591, found 415.2601 (δ + 2.43 ppm).

6.11. (3aS,7aR)-N-[3-Methyl-1S-(3-oxo-hexahydro-furo[3,2-b]pyridine-4-carbonyl)-butyl]-4-(4-methyl-piper-azin-1-yl)benzamide (46)

HPLC t_R = 11.9 min (98%), HPLC–MS 457.3 [M + H]$^+$. Exact mass calcd for $C_{25}H_{36}N_4O_4$ (MH$^+$): 457.2809, found 457.2830 (δ + 4.55 ppm).

6.12. (2R,3S)-4-tert-Butyl-N-[3-methyl-1-(2-methyl-4-oxo-tetrahydrofuran-3-yl-carbamoyl)butyl]benzamide (49a)[36]

HPLC t_R = 19.1 min (93%), HPLC–MS 389.3 [M + H]$^+$, 799.5 [2M + Na]$^+$. Exact mass calcd for $C_{22}H_{32}N_2O_4$ (MH$^+$): 389.2435, found 389.2442 (δ + 1.93 ppm).

6.13. (2R,3S)-N-[3-Methyl-1S-(2-methyl-4-oxo-tetra-hydrofuran-3-ylcarbamoyl)-butyl]-4-(4-methyl-piperazin-1-yl)benzamide (49b)[36]

HPLC t_R = 10.2 min (97%), HPLC–MS 431.3 [M + H]$^+$, 883.5 [2M + Na]$^+$. Exact mass calcd for $C_{23}H_{34}N_4O_4$ (MH$^+$): 431.2653, found 431.2673 (δ + 4.71 ppm).

Additionally, analogue **10** was prepared on a 50 μM scale (5 × 10 μM crowns) and purified over silica (20 g) eluting with a gradient of heptane–ethyl acetate 1:1 → 1:3. Desired fractions were combined and reduced in vacuo to a white solid (8.0 mg, 40%). TLC (single UV spot, R_f = 0.55, heptane–ethyl acetate 1:1), analytical HPLC Rt = 17.6 min, HPLC–MS (single UV peak with t_R = 10.3–11.1 min, 401.2 [M + H]$^+$, 419.2 [M + H + 18]$^+$, 423.2 [M + Na]$^+$). ^{1}H NMR (500 MHz, CDCl$_3$ at 298 K): δ 0.92 (d, J = 6.50 Hz, Leu CHC$H_{3\delta}$, 3H), 1.02 (d, J = 6.45 Hz, Leu CHC$H_{3\delta'}$, 3H), 1.32 (s, C(CH_3)$_3$, 9H), 1.58–1.80 (m, Leu C$H_{2\beta}$ + CH_γ, 3H), 2.00–2.14/2.18–2.34 (m, NCH$_2$CH_2, 2H), 3.55–3.65 (m, NCH_2CH$_2$, 1H), 3.98 (d, J = 17.00 Hz, COCH_{2A}, 1H), 4.14 (d, J = 17.30 Hz, COCH_{2B}, 1H), 4.10–4.30 (m, NCH_2CH$_2$, 1H), 4.67 (d, J = 5.10 Hz, CH_α, 1H), 4.91 (m, CH_β, 1H), 5.02–5.11 (m, Leu CH_α, 1H), 6.91 (br d, NH), 7.43 (d, J = 8.30 Hz, CH–CCONH, 2H$_{aromatic}$), 7.73 (d, J = 8.35 Hz, C(CH$_3$)$_3$–CCH, 2H$_{aromatic}$); ^{13}C NMR (125 MHz, CDCl$_3$ at 298 K): δ 21.94 (Leu $C_{3\delta}$), 23.60 (Leu $C_{3\delta}$), 24.80 (Leu C_γ), 29.67 (C(C_3)$_3$), 32.48 (NCH$_2$$CH_2$), 42.59 (Leu CH$_{2\beta}$), 45.61 (NCH$_2CH_2$), 49.64 (Leu C_α), 62.17 (C_α), 71.03 (COCH$_2$), 80.75 (C_β), 125.34/125.50 (C(CH$_3$)$_3$–CCH, C(CH$_3$)$_3$–CCH′, 2C$_{aromatic}$), 126.91/127.0 (C(CH$_3$)$_3$–CCHCH, C(CH$_3$)$_3$–CCHCH′, 2C$_{aromatic}$), 130.87 (C–CONH$_{aromatic}$), 155.30 (C(CH$_3$)$_3$$CCH_{aromatic}$), 167.03 ($C$ONH), 172.22

(Leu CON), 208.36 (COCH$_2$). This batch of **10** was used for DMPK and cell-based protocols.

6.14. Assays for cysteinyl proteinase activity

Stock solutions of substrate or inhibitor were made up to 10 mM in 100% dimethylsulfoxide (DMSO) (Rathburns, Glasgow, U.K.) and diluted as appropriately required. In all cases the DMSO concentration in the assays was maintained at less than 1% (vol/vol). The equilibrium inhibition constants (K_i^{ss}) for each compound were measured under steady-state conditions monitoring enzyme activity as a function of inhibitor concentration. The values were calculated on the assumption of pure competitive behaviour.[45] Assay protocols were based on literature precedent (Barrett, Rawlings, and Woessner, 1998, *Handbook of Proteolytic Enzymes*, Academic Press, London and references therein) and modified as required to suit local assay protocols.[8a,b]

6.15. Measurement of inhibitor on-rates and off-rates

The observed rates of reaction for the association of compound with enzyme (k_{on}) and for the dissociation of compound from enzyme (k_{off}) were analysed as previously described.[7] Recombinant human cathepsin K was assayed in 100 mM sodium acetate; pH 5.5; 1 mM EDTA; 10 mM L-cysteine, 0.05% Tween 20 employing 1.5 μM (equal to K_M^{app}) Z-Leu-Arg-AMC as the substrate.[46] For measurements of the association rates, assays were carried out by addition of various concentrations of inhibitor to assay buffer containing substrate and initiated by the addition of enzyme. For the measurements of dissociation rates, pre-incubated enzyme plus inhibitor were diluted at least 20-fold into assay buffer containing substrate. During the course of the assay less than 10% of the substrate was consumed and the observed rates corrected for substrate kinetics.

6.16. Measurement of bone resorption activity

Bone resorption assays were carried out as a service by Pharmatest Services Ltd, Itäinen Pitkäkatu 4, 20520 Turku, Finland. Bone resorption was studied using a model where human osteoclast precursor cells derived from peripheral blood were cultured on bovine bone slices for nine days and allowed to differentiate into bone-resorbing osteoclasts, and the formed mature osteoclasts were then allowed to resorb bone. After the culture period, collagen fragments (CTX) released from the bone slices during the culture period were determined using CrossLaps® for culture assay (Nordic Bioscience, Herlev, Denmark). A baseline group without test compound was included providing a negative control. Additionally, a positive control E-64, an inhibitor of cathepsin enzymes and osteoclastic bone resorption, was used to demonstrate that the test system was able to detect inhibition of bone resorption. Compound **10** was added to the test culture media at 10, 1 and 100 nM ($n = 6$ replicates).

References and notes

1. (a) Otto, H.-H.; Schirmeister, T. *Chem. Rev.* **1997**, *97*, 133; (b) Veber, D. F.; Thompson, S. K. *Curr. Opin. Drug Discov. Dev.* **2000**, *3*, 362–369.
2. (a) Chapman, H. A.; Riese, R. J.; Shi, G.-P. *Annu. Rev. Physiol.* **1997**, *59*, 63; (b) Lecaille, F.; Kaleta, J.; Brömme, D. *Chem. Rev.* **2002**, *102*, 4459; (c) Brömme, D.; Kaleta, J. *Curr. Pharm. Des.* **2002**, *8*, 1639–1658.
3. Barrett, A. J.; Rawlings, N. D.; Woessner, J. F. *Handbook of Proteolytic Enzymes*; Academic: New York, 1998.
4. (a) Thornberry, N. A. *Chem. Biol.* **1998**, *5*(5), R97–R103; (b) Leung-Toung, R.; Li, W.; Tam, T. F.; Karimian, K. *Curr. Med. Chem.* **2002**, *9*, 979; (c) Hernandez, A. A.; Roush, W. R. *Curr. Opin. Chem. Biol.* **2002**, *6*, 459; (d) Kim, W.; Kang, K. *Expert Opin. Ther. Patents* **2002**, *12*(3), 419.
5. Watts, J.; Benn, A.; Flinn, N.; Monk, T.; Ramjee, M.; Ray, P.; Wang, Y.; Quibell, M. *Bioorg. Med. Chem.* **2004**, *12*, 2903.
6. (a) Marquis, R. W.; Ru, Y.; Zeng, J.; Lee Trout, R. E.; LoCastro, S. M.; Gribble, A. D.; Witherington, J.; Fenwick, A. E.; Garnier, B.; Tomaszek, T.; Tew, D.; Hemling, M. E.; Quinn, C. J.; Smith, W. W.; Zhao, B.; McQueney, M. S.; Janson, C. A.; D'Alessio, K.; Veber, D. F. *J. Med. Chem.* **2001**, *44*, 725, and references cited therein; (b) Marquis, R. W.; Ru, Y.; LoCastro, S. M.; Zeng, J.; Yamashita, D. S.; Oh, H.-J.; Erhard, K. F.; Davis, L. D.; Tomaszek, T. A.; Tew, D.; Salyers, K.; Proksch, J.; Ward, K.; Smith, B.; Levy, M.; Cummings, M. D.; Haltiwanger, R. C.; Trescher, G.; Wang, B.; Hemling, M. E.; Quinn, C. J.; Cheng, H.-Y.; Lin, F.; Smith, W. W.; Janson, C. A.; Zhao, B.; McQueney, M. S.; D'Alessio, K.; Lee, C.-P.; Marzulli, A.; Dodds, R. A.; Blake, S.; Hwang, S.-M.; James, I. E.; Gress, C. J.; Bradley, B. R.; Lark, M. W.; Gowen, M.; Veber, D. F. *J. Med. Chem.* **2001**, *44*, 1380, and references cited therein; (c) Fenwick, A. E.; Gribble, A. D.; Ife, R. J.; Stevens, N.; Witherington, J. *Bioorg. Med. Chem. Lett.* **2001**, *11*, 199.
7. (a) Morrison, J. F.; Walsh, C. T. *Adv. Enzymol. Relat. Areas Mol. Biol.* **1988**, *61*, 201; (b) Tian, W. X.; Tsou, C. L. *Biochemistry* **1982**, *21*(5), 1028.
8. See: (a) Quibell, M. Patent WO 02/057270; (b) Quibell, M.; Ray, P. C.; Watts, J. P. Patent WO 04/007501.
9. (a) Eliel, E. L.; Wilen, S. H.; Mander, L. N. In *Stereochemistry of Organic Compounds*; Wiley: New York, 1994; pp 1–1267; (b) Eliel, E. L. In *Stereochemistry of Carbon Compounds*; McGraw-Hill: New York, 1962; pp 1–486.
10. (a) Blomquist, A. T.; Kwiatek, J. *J. Am. Chem. Soc.* **1951**, *73*, 2098; (b) Mann, G. *Z. Chem.* **1966**, *6*(3), 106; (c) Reppe, W.; Schlichting, O.; Klager, K.; Toepel, T. *Liebigs Ann. Chem.* **1948**, *560*, 1; (d) Spelbos, A.; Mijlhoff, F. C.; Bakker, W. H.; Baden, R.; Van den Enden, L. *J. Mol. Struct.* **1977**, *38*, 155; (e) Allinger, N. L.; Nakazaki, M.; Zalkow, V. *J. Am. Chem. Soc.* **1959**, *81*, 4074; (f) Barrett, J. W.; Linstead, R. P. *J. Chem. Soc.*, **1936**, 611;

(g) Browne, C. C.; Rossini, F. D. *J. Phys. Chem.* **1960**, *64*, 927.

11. (a) Salomon, R. G.; Coughlin, D. J.; Ghosh, S.; Zagorski, M. G. *J. Am. Chem. Soc.* **1982**, *104*(4), 998; (b) Owsley, D. C.; Bloomfield, J. J. *J. Chem. Soc. Sect. C* **1971**, *20*, 3445; (c) No references are found for *cis* or *trans*-bicyclo[5.2.0]nonan-6-one although a CAS registry is present 105104-52-7.

12. No references are found for *trans*-bicyclo[3.3.0]octan-2-one whilst the *cis* isomer is well known, for example, see: Cope, A. C.; Lee, H. H.; Petree, H. E. *J. Am. Chem. Soc.* **1958**, *80*, 2849.

13. (a) Allinger, N. L.; Tribble, M. T. *Tetrahedron* **1972**, *28*, 1191; (b) Brown, H. C.; Negishi, E. *J. Chem. Soc., Chem. Commun.* **1968**, 594; (c) House, H. O.; Rasmusson, G. H. *J. Org. Chem.* **1963**, *28*, 31; (d) Boger, D. L.; Mathvink, R. J. *J. Org. Chem.* **1988**, *53*, 3379.

14. (a) Concannon, P. W.; Ciabattoni, J. *J. Am. Chem. Soc.* **1973**, *95*(10), 3284, and references cited therein; (b) Dhokte, U. P.; Pathare, P. M.; Mahindroo, V. K.; Brown, H. C. *J. Org. Chem.* **1998**, *63*, 8276.

15. Energy calculations were performed on each carbocycle, both in *cis* and *trans*-fused geometry, then the process repeated by stepwise addition of the α sp^2 ketone carbonyl, heteroatoms as appropriate, the enol intermediate and finally through *si* and *re* stereofacial addition of methanethiol as a model of the proteinase bound intermediate hemithioketal. Each compound was generated in ChemDraw Ultra (v6.0, CambridgeSoft Corp.), then copy and pasted into Chem3D Pro (v5.0, CambridgeSoft Corp.) for an MM2 energy minimisation (RMS gradient = 0.1). The 'total energy' was then calculated for each minimised conformer, which relates to the total steric energy of the conformation and hence the relative stability of the conformer.

16. It cannot be assumed that the literature detailed relative stabilities for carbocycle and ketocarbocycles are conserved upon the introduction of the heteroatoms into ketoheterocycles **4**–**8**. Indeed, literature shows that certain heterocyclic analogues of bicyclo[3.3.0]octane exist in both *cis* and *trans*-fused conformations exist, for example, see: Owen, L. N.; Peto, A. G. *J. Chem. Soc.* **1955**, 2383.

17. A clear example of the point made in Ref. 16 is shown by the stable 5,5-bicycle detailed by GSK that is *trans*-fused and provides a generalised scaffold for serine protease inhibition. However, this scaffold does not contain a ketone functionality α to either bridgehead position and as such does not have a facile mechanism for loss of chirality through enolisation. See: Borthwick, A. D.; Angier, S. J.; Crame, A. J.; Exall, A. M.; Haley, T. M.; Hart, G. J.; Mason, A. M.; Pennell, A. M. K.; Weingarten, G. G. *J. Med. Chem.* **2000**, *43*, 4452.

18. For example; (a) Cathepsin, K.; McGrath, M. E.; Klaus, J. L.; Barnes, M. G.; Brömme, D. *Nat. Struct. Biol.* **1997**, *4*(2), 105; (b) Cathepsin, K.; Tavares, F. X.; Boncek, V.; Deaton, D. N.; Hassell, A. M.; Long, S. T.; Miller, A. B.; Payne, A. A.; Miller, L. R.; Shewchuk, L. M.; Wells-Knecht, K.; Willard, D. H., Jr.; Wright, L. L.; Zhou, H.-Q. *J. Med. Chem.* **2004**, *47*, 588; (c) Cathepsin, S.; McGrath, M. E.; Palmer, J. T.; Brömme, D.; Somoza, J. R. *J. Prot. Sci.* **1998**, *7*, 1294; (d) Cathepsin, F.; Somoza, J. R.; Palmer, J. T.; Ho, J. D. *J. Mol. Biol.* **2002**, *322*, 559; (e) Cathepsin, V.; Somoza, J. R.; Zhan, H.; Bowman, K. K.; Yu, L.; Mortara, K. D.; Palmer, J. T.; Clark, J. M.; McGrath, M. E. *Biochemistry* **2000**, *39*, 12543; (f) Cathepsin, B.; Greenspan, P. D.; Clark, K. L.; Tommasi, R. A.; Cowen, S. D.; McQuire, L. W.; Farley, D. L.; van Duzer, J. H.; Goldberg, R. L.; Zhou, H.; Du, Z.; Fitt, J. J.; Coppa, D. E.; Fang, Z.; Macchia, W.; Zhu, L.; Capparelli, M. P.; Goldstein, R.; Wigg, A. M.; Doughty, J. R.; Bohacek, R. S.; Knap, A. K. *J. Med. Chem.* **2001**, *44*(26), 4524.

19. Desjarlais, R. L.; Yamashita, D. S.; Oh, H.-J.; Uzinskas, I. N.; Erhard, K. F.; Allen, A. C.; Haltiwanger, R. C.; Zhao, B.; Smith, W. W.; Abdel-Meguid, S. S.; D'Alessio, K.; Janson, C. A.; McQueney, M. S.; Tomaszek, T. A.; Levy, M. A.; Veber, D. F. *J. Am. Chem. Soc.* **1998**, *120*, 9114.

20. A further example of the deleterious effects of P1 inhibitor secondary amide *N*-methylation is provided in Ref. 19. However, here only a fourfold loss in potency was observed, but this effect is detailed in a symmetrical inhibitor, which may potentially bind is a reverse manner, placing the *N*-methylated residue in an alternative proteinase binding pocket.

21. For example see PDB codes, cathepsin K 1au0 (*cis*), 1au2 (*cis*), 1bgo (*trans*), 1mem (*trans*), 1nl6 (*cis*), 1nj7 (*cis*); cathepsin S 1ms6 (*cis*), 1npz (*cis*); cathepsin V 1fh0 (*trans*); cruzain 1aim (*cis*).

22. In-house molecular modelling was performed as previously described (Ref. 5) using WebLab ViewerPro (http://www.accelrys.com). The literature cathepsin K X-ray crystal structures 1mem (nonprime orientations) and 1au0 (prime and nonprime orientations) were used as templates to examine the general overall spatial fit and potential binding orientations of heterobicyclic scaffolds **4** and **5**. The existing inhibitors bound within 1mem and 1au0 were modified into the desired bicyclic compounds **10** and **11** by simple draw and clean commands whilst retaining as close as possible the main thread of the inhibitor backbone. A hemithioketal tetrahedral intermediate formed between the bicyclic ketone carbonyl and the active site Cys^{25} was built to examine the products of both *re* and *si* stereofacial addition of the thiolate. As part of the assessment, calculations were performed on the isolated hemithioketal tetrahedral intermediate extracted from the predicted bound complex, to ascertain whether the binding model contained a reasonable energy inhibitor conformation. Conformer energy calculations were performed using CAChe (Conflex molecular mechanics engine, CAChe Group, Fujitsu). Additionally, the full modelling process considering each possible binding orientation was repeated using the literature cruzain X-ray structure 1aim and the mammalian cathepsin S X-ray structure 1ms6. Virtually identical conclusions concerning the preferred binding orientations described herein for the cathepsin K 1mem and 1au0 structures were found when substituting with the 1aim and 1ms6 structures.

23. Predictions of likely binding conformations were performed as previously described (Ref. 5) and based solely upon comparison of the four possible *re/si*/prime side/nonprime side complexes for each bicycle. Major considerations in the development of a ranking for each possibility were the identification of a reasonable energy conformer for the inhibitor that retained a good hydrogen bonding network to the proteinase along with the absence of spatial clashes. The overall goodness of fit was assessed using the scoring functions generated by the software package 'GOLD 2.1' (Cambridge Crystallographic Data Centre) performing the calculations on the tetrahedral intermediates.

24. Veber, D. F.; Johnson, S. R.; Cheng, H.-Y.; Smith, B. R.; Ward, K. W.; Kopple, K. D. *J. Med. Chem.* **2002**, *45*, 2615.

25. Wisniewski, K.; Koldziejczyk, A. S.; Falkiewicz, B. *J. Pept. Sci.* **1998**, *4*(1), 1.

26. Kolodziej, S. A.; Marshall, G. R. *Int. J. Pept. Prot. Res.* **1996**, *48*(3), 274.

27. [13]C chemical shifts (CDCl$_3$ at 298 K) gave C-*2* (compound **16** at 68.32/68.72 ppm, compound **18** at 63.89/64.22 ppm) and C-*3* (compound **16** at 74.49/75.67 ppm, compound **18** at 71.84/72.80 ppm) in comparison to those of the analogous literature Nα-*tert*-butoxycarbonyl-3-hydroxyproline methyl esters[26] (*trans* giving C-*2* at 67.7/67.9 and C-*3* at 74.0/75.1 ppm; *cis* giving C-*2* at 63.3/64.0 and C-*3* at 71.3/72.0 ppm).

28. Dessolin, M.; Guillerez, M.-G.; Thieriet, N.; Guibe, F.; Loffet, A. *Tetrahedron Lett.* **1995**, *36*(32), 5741.

29. For a general synthesis of Fmoc-aminoacid chloromethylketones from the corresponding diazomethylketones, see: Wood, J. L.; Huang, L.; Ellman, J. A. *J. Comb. Chem.* **2003**, *5*, 869.

30. Drummond, J.; Johnson, G.; Nickell, D. G.; Ortwine, D. F.; Bruns, R. F.; Welbaum, B. *J. Med. Chem.* **1989**, *32*, 2116.

31. Scott, J. D.; Williams, R. M. *Tetrahedron Lett.* **2000**, *41*, 8413.

32. The synthetic details in Scheme 2 were repeated to convert alcohol (+)-(2*R*,3*S*)-**30** sequentially into the corresponding compounds; *tert*-butyl ether protected analogue (−)**39** (74.3%) ($[\alpha]_D^{22}$ − 20.7 (*c* 0.314, CHCl$_3$)); Free acid (−)**40** (82.3%). Microanalysis indicated the presence of residual solvent following drying in vacuo and re-drying at elevated temperature lead to partial thermal decomposition. Exact mass calcd for C$_{25}$H$_{29}$NO$_5$ (MNa$^+$): 446.1938, found 446.1948 (δ +2.25 ppm); $[\alpha]_D^{22}$ − 19.4 (*c* 0.423, CHCl$_3$). Diazomethylketone **41** with analytical HPLC t_R = 18.8 min, HPLC–MS (UV peaks with t_R = 9.1 min, 364.2 [M + H]$^+$, 386.1 [M + Na]$^+$, 749.2 [2M + Na]$^+$ and t_R = 10.9 min, 420.2 [M + H − N$_2$]$^+$, 470.2 [M + Na]$^+$, 917.3 [2M + Na]$^+$), note that upon HPLC–MS analysis, *m/z* 364.2 *apparently* corresponds to the bicycle product; 6,5-bicycle (+)-(3a*R*,7a*S*)-**42** (overall 47.7% from acid **40**). Microanalysis indicated the presence of residual solvent following drying in vacuo and re-drying at elevated temperature lead to partial thermal decomposition. Exact mass calcd for C$_{22}$H$_{21}$NO$_4$ (MH$^+$): 364.1543, found 364.1553 (δ +2.66 ppm); $[\alpha]_D^{22}$ + 14.3 (*c* 0.308, CHCl$_3$). Compounds (−)**39**, (−)**40**, **41** and (+)**42** are enantiomers of the fully detailed compounds (+)**33**, (+)**34**, **35** and (−)**13** and exhibited virtually identical NMR spectra to those annotated herein. Preparation of (−)**39**, (−)**40**, **41** and (+)**42** are unpublished syntheses, although see Ref. 8a for preliminary disclosure.

33. Murphy, A. M.; Dagnino, R.; Vallar, P. L.; Trippe, A. J.; Sherman, S. L.; Lumpkin, R. H.; Tamura, S. Y.; Webb, T. R. *J. Am. Chem. Soc.* **1992**, *114*, 3156.

34. For a thorough description of general multipin techniques, see: Grabowska, U.; Rizzo, A.; Farnell, K.; Quibell, M. *J. Comb. Chem.* **2000**, *2*(5), 475.

35. (a) In general, the quality of crude examples ranged from 50% to >80% as judged by analytical HPLC. Under the strong acidolytic cleavage conditions required to release compounds **10**, **45a–e** and **11**, **46** from the solid phase we observed that a side-product consisting of R^{3}CON-HCHR^2-COOH could be observed in most crude examples. This side-product, that derives from cleavage of the 3° amide bond, was readily removed by semi-preparative HPLC; (b) Appearance of the same R^{3}CON35HCHR^2-COOH product was the major mechanism of compound instability when assessed under acid, neutral and basic buffered conditions.

36. Monocyclic analogues such as **49a,b** were prepared for comparison following the general methods detailed in Quibell, M.; Taylor, S. Patent WO 00/69855.

37. We are unable to further rationalise such a clear experimental result using the simple design tools and techniques described herein (Refs. 22,23).

38. Stroup, G. B.; Lark, M. W.; Veber, D. F.; Bhattacharyya, A.; Blake, S.; Dare, L. C.; Erhard, K. F.; Hoffman, S. J.; James, I. E.; Marquis, R. W.; Ru, Y.; Vasko-Moser, J. A.; Smith, B. R.; Tomaszek, T.; Gowen, M. *J. Bone Miner. Res.* **2001**, *16*(10), 1739.

39. We were unable to follow the stability of analogues **10** and **45a**[6b,c] by chiral HPLC due to the earlier described broad elution profile and our failure to prepare the authentic *trans* standard for comparison. However, all our evidence, build upon the assumption that the *cis* and *trans*-fused diastereoisomers would show different and separable physical properties, gave no evidence for loss of α-chirality. For example, analogue **10** was prepared by the solid phase methods described herein on a 50 μM scale and purified by standard silica chromatography. TLC analysis of purified **10** exhibited a single tight UV positive spot that remained unchanged after three days in a range of organic and mixed organic/aqueous buffers. Additionally, NMR analysis of analogue **10** showed no evidence for the *trans* 5,5-bicycle even upon prolonged dissolution in NMR solvents. Broadly similar finding were evident for the corresponding 6,5-bicycle analogue **11**.

40. Lipinski, C. A.; Lombardo, F.; Dominy, B. W.; Feeney, P. J. *Adv. Drug Deliver. Rev.* **1997**, *23*, 3.

41. Riley, R. J. *Curr. Opin. Drug Discovery Dev.* **2001**, *4*(1), 45.

42. James, I. E.; Dodds, R. A.; Olivera, D. L.; Nuttall, M. E.; Gowen, M. *J. Bone Miner. Res.* **1996**, *11*, 1453.

43. Atherton, E.; Sheppard, R. C. In *Solid Phase Peptide Synthesis A Practical Approach*; IRL: Oxford, U.K., 1989.

44. Meldal, M.; Breddam, K. *Anal. Biochem.* **1991**, *195*, 141.

45. Cornish-Bowden, A. *Fundamentals of Enzyme Kinetics*; Portland: London, 1995.

46. Bossard, M. J. *J. Biol. Chem.* **1996**, *271*(21), 12517.